TWO-DIMENSIONAL INTERPRETATION OF SCHLUMBERGER SOUNDINGS AND HEAD-ON DATA WITH EXAMPLES FROM EYJAFJORDUR ICELAND, AND OLKARIA, KENYA

Martin N. Mwangi*
UNU Geothermal Training Programme,
National Energy Authority,
Grensasvegur 9, 108 Reykjavik, Iceland.

*
Permanent address:
East African Power and Lighting Company,
Geothermal Section,
P.O. Box 30099, Nairobi, Kenya.

ABSTRACT

The theory of resistivity soundings and interpretation in geothermal exploration over two-dimensional half-space is discussed. The basic principles of the head-on method are reviewed and some theoretical models presented. These models include low and high resistivity dikes, vertical contacts and a dipping low resistivity dike. The effect of burying a low resistivity dike at different depths and a structure with the uppermost layer having a vertical contact were studied. These models are very important type structures in geothermal fields and could help in the exploration for permeable zones. The head-on method detects such structures more easily than classical methods.

Some resistivity data from Eyjafjordur in Iceland were interpreted in one- and two-dimensions. In Eyjafjordur valley, sediments with resistivities in the range of 3-5 ohmm and about 175m thick occur at the bottom of the valley and extend about 300m in the E-W direction. They are underlain by a substratum with a resistivity of about 150-380 ohmm. The resistivity of the substratum is in general lower (about 150 ohmm) east of the valley.

Head-on data from the Olkaria geothermal field, Kenya, was successfully interpreted two-dimensionally. This was intergreted with Schlumberger soundings and gravity data. A thin vertical structure with a resistivity of about 1 ohmm was revealed. The structure was not evident from the gravity data. It is possible that this structure is the conduit for some weak fumaroles in the vicinity of the resistivity profile. This work demonstrates that the head-on data which could not previously be interpreted quantitatively can be successfully interpeted by computer modelling. An interpretation of the data south of the present profile should facilitate the mapping of this vertical structure. This should greatly assist in the siting of more productive boreholes in this area.

TABLE OF CONTENTS

LIST OF FIGURES

1 INTRODUCTION

1.1 Scope of work

This report is a part of the work undertaken by the author during six months training at the UNU Geothermal Training Programme attended by the author in Iceland under the sponsorship of the United Nations University and the Icelandic government in 1982.

The training started by 5 weeks of introductory lectures and seminars on geology, exploration geophysics, borehole geophysics, geochemistry, groundwater hydrology, reservoir engineering, drilling and geothermal utilization.

The author received specialized training for 2 months in collecting and interpreting Schlumberger soundings, head-on, gravity and magnetic data. He also went on a 2-week field excursion to the main low and high temperature areas of Iceland.

This report consists of theoretical model studies on the head-on method and two-dimensional interpretations of Schlumberger soundings and head-on data from Eyjafjordur, Iceland and Olkaria, Kenya, respectively. The work was done as a project in the last two and a half months of the training programme.

1.2 Introduction to resistivity interpretation

Until recently most DC apparent resistivity curves have in geophysical exploration been interpreted assuming a horizontally layered earth free from inhomogeneities. This was because the master curves and one-dimensional (1-D) computer interpretations methods were based upon horizontally layered models of infinite lateral extents. There existed no sound interpretation procedure of interpreting apparent resistivity curves strongly affected

by lateral resistivity changes due to faults or irregularly shaped bodies. However, resistivity curves for simple models from mathematical computation and scaled model experiments have been published (McPhar Geophysics,1967; Apparao et al., 1969).

Faults and irregularly shaped bodies are very common in geothermal areas. Low resistivity bodies caused by deep hydrothermal alterations are fairly irregular in such cases. Volcanic plugs , dykes and lava flows are generally of finite extents and in earlier years there were no ways of allowing for this in the one dimension interpretation.

Dey and Morrison (1977) published an algorithm for computing the apparent resistivity from 2-D structures of infinite extents in the strike direction. The algorithm solves simultaneously some finite difference equations of potential distribution on the surface of a half-space due to point current sources. The 2-D computer program of Dey (1976) based on the finite difference algorithm was used by Beyer (1977) to compute the apparent resistivities for 2-D models of several configurations.

During the author's training the 2-D program by Dey (1976) was used to interpret some Schlumberger resistivity soundings from Akureyri,N-Iceland. The 2-D program has been modified at the National Energey Authority of Iceland to compute the head-on resistivity. The program was also used to interpret head-on data collected by the author in Olkaria geothermal field, Kenya, and to compute some theoretical models discussed in section 4 of this report. This work is described in the report.

2. THEORY OF RESISTIVITY INTERPRETATION

2.1 Introduction

In the electrical methods, where current is driven into the ground through electrodes, any subsurface variation in conductivity alters the form of the current flow in the earth and this affects the distribution of the electric potential. The degree to which the potential at the surface is affected depends on the size, shape, location and the electrical resistivity of the subsurface masses. It is therefore possible to obtain information about the distribution of these bodies both vertically and laterally from the potential measurements made at the surface. The parameter determined from the measured potential distribution is the apparent resistivity.

2.2 Determination of apparent resistivity

A positive current I is driven into the ground through a current electrode A and a negative current comes out through electrode B. A potential difference, V, is measured between two points M and N at the surface of the earth. The apparent resistivity is given by

$$\rho_a = \frac{\Delta V}{I} G \qquad (2.1)$$

where for general configuration in Fig.(2.1),

$$G = 2\pi \frac{1}{\left(\frac{1}{r_1} - \frac{1}{r_2} - \frac{1}{r_3} + \frac{1}{r_4}\right)}$$

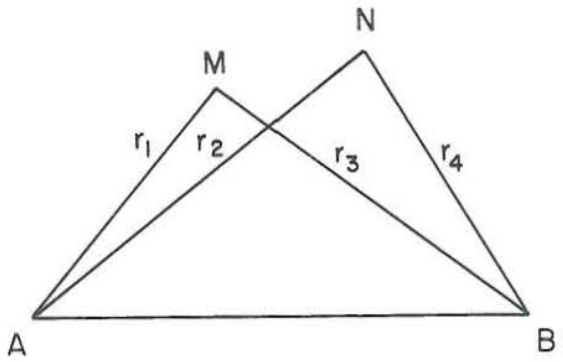

Fig. 2.1 Electrode array for an arbitrary geometric factor

2.3 Resistivity sounding with Schlumberger array

The Schlumberger configuration shown in Fig.(2.2) can be used to determine the apparent resistivity values as a function of the distance AB which is succesively increased. This is called resistivity sounding and the resistivity change below the centre of the configuration can be found. The apparent resistivity values are plotted against the AB/2 in a log-log paper.

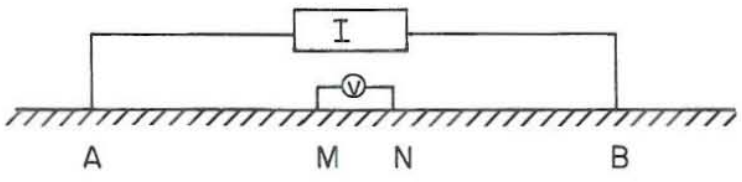

Fig. 2.2 Schlumberger array

If the half-space consists of a homogeneous and isotropic single layer of infinite thickness, the sounding curve will be a straight line of apparent resistivity equal to the true resistivity. In many cases the assumption is that the half-space consists of many layers each having a different resistivity and finite thickness. In that case the apparent resistivity curves can be interpreted using master curves and/or auxiliary point graphs and by automatic or non-automatic computer iteration techniques (Johansen, 1975; Koefoed, 1979). These methods are based on the following assumptions:

(1) The subsurface consists of horizontal strata separated by horizontal boundary planes,the thickness of the deepest layer is infinite and all the other layers have finite thicknesses.

(2) Each of the layers is electrically homogeneous and isotropic.

2.4 Sounding over non-horizontal earth

The effects of dipping and vertical contacts and inhomogeneities depend on the size,location relative to the sounding centre and the resistivity contrasts. The biggest problem in the interpretation of curves with these effects has been the difficulty in the mathematical formulation of potential caused by the irregularly shaped bodies. Great efforts are being put towards finding these mathematical formulations (Lee, 1981). Studies have been limited to very simple structures owing to the above problem.

Van Nostrand and Cook (1955), De Gery and Kunetz(1956) and others have published master curves over simple structures using the method of images proposed by Unz (1953). Tank model experiments have also been used (McPhar Geophysics, 1967). However, it is practically difficult to find a very homogeneous material easy to work with and for which one

can vary the resistivity conviniently through the necessary range. In practice, soundings in tank models have also been limited to a few cases such as vertical or dipping faults in the overburden overlying an infinitely resistant basement.

2.4.1 Dipping contacts

Fig.(2.3) shows the apparent resistivity curves which would be obtained by a Schlumberger array expanded parallel to the dipping contact and over horizontal layers of the same resistivity contrast.The shape of the curve does not appear different from those of the horizontal layers except the curvature of the dipping model is more.

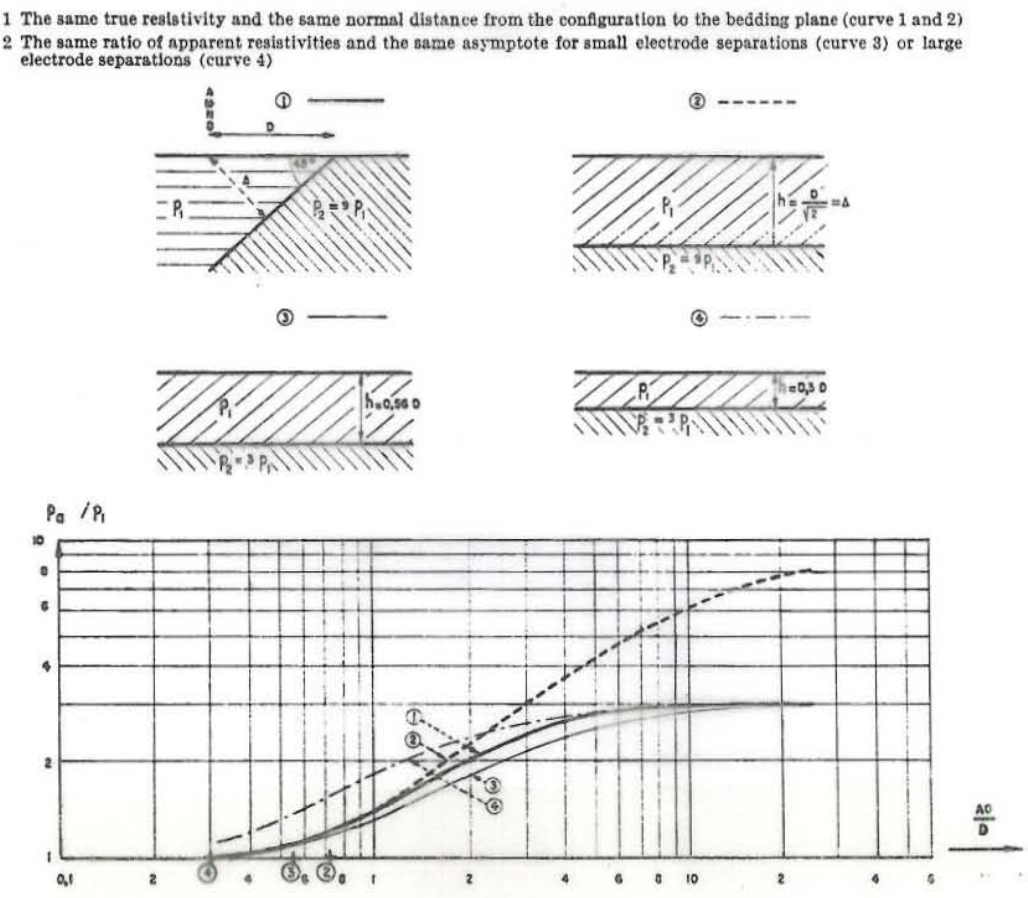

Fig. 2.3 Resistivity soundings made with array parallel to a dipping contact and over horizontal layers (from Kunetz, 1966)

This curvature increases with the increase in the angle of dip. For dips less than 10 degrees, the effect is small and can be ignored (Koefoed, 1979).

For a configuration oriented perpendicular to the contact, the curves show sharp discontinuities. Fig.(2.4) shows some typical curves depending on the distance between the sounding centre and the contact. In Fig.(2.4a) where the centre of the array is downdip and $\rho_1 < \rho_2$ the apparent resistivity increases much faster. This is because the current is concentrated in the low resistivity layer (more conductive) as the resistive layer reduces the flow beyond the contact. When one current electrode crosses the contact, the resistivity starts to decrease and then rises gradually.

2.4.2 Vertical contacts

Vertical contacts as created by faults are quite common in geothermal areas. The strongest effects are again realized when the profiles are oriented perpendicular and close to the structures (Fig.2.5). When the centre is in the low resistivity layer, the curve rises steeply, sometimes exceeding the limiting 45 degrees slope both in the parallel and perpendicular soundings. The perpendicular soundings will show a sharp break as the current electrode is positioned at the contact. It is important to note that these breaks are less conspicuos if the contacts are buried at depths by the overlying layers and also when the resistivities have little contrast.

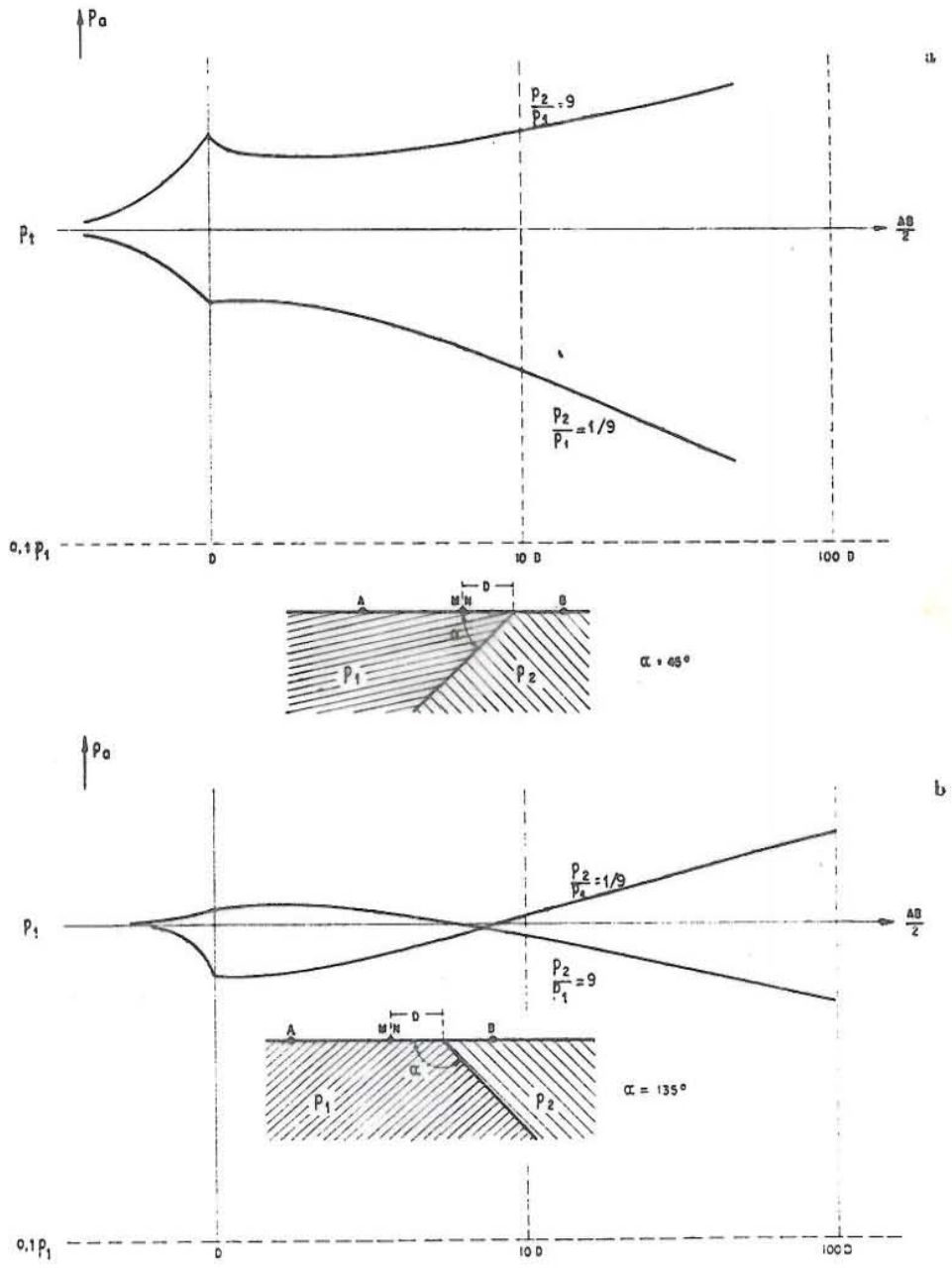

Fig. 2.4 Resistivity soundings made with an array perpendicular to the strike of the dipping contact (from Kunetz, 1966)

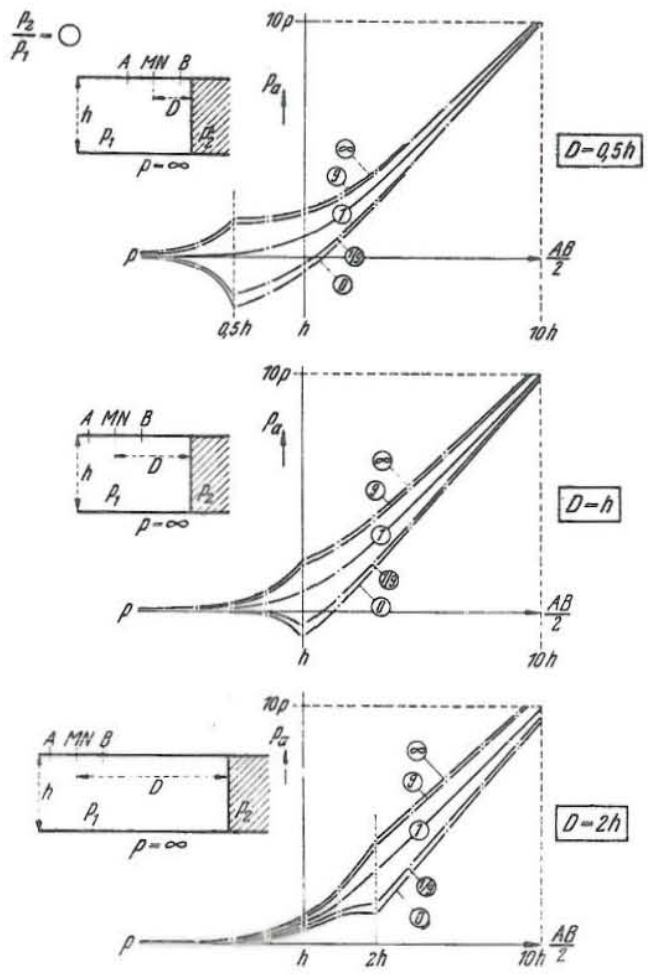

Fig. 2.5 Resistivity curves near a vertical contact underlain by an infinitely resistant substratum (from Kunetz, 1966).

2.4.3 A thin vertical dike

A thin vertical dike, even when it has a highly contrasting resistivity to the host rock will not effect any change in the sounding parallel to it. On the other hand, a resistant dike causes a steep slope in the the first part of the curve and a vertical discontinuity as soon as the electrode crosses it (Fig.2.6).

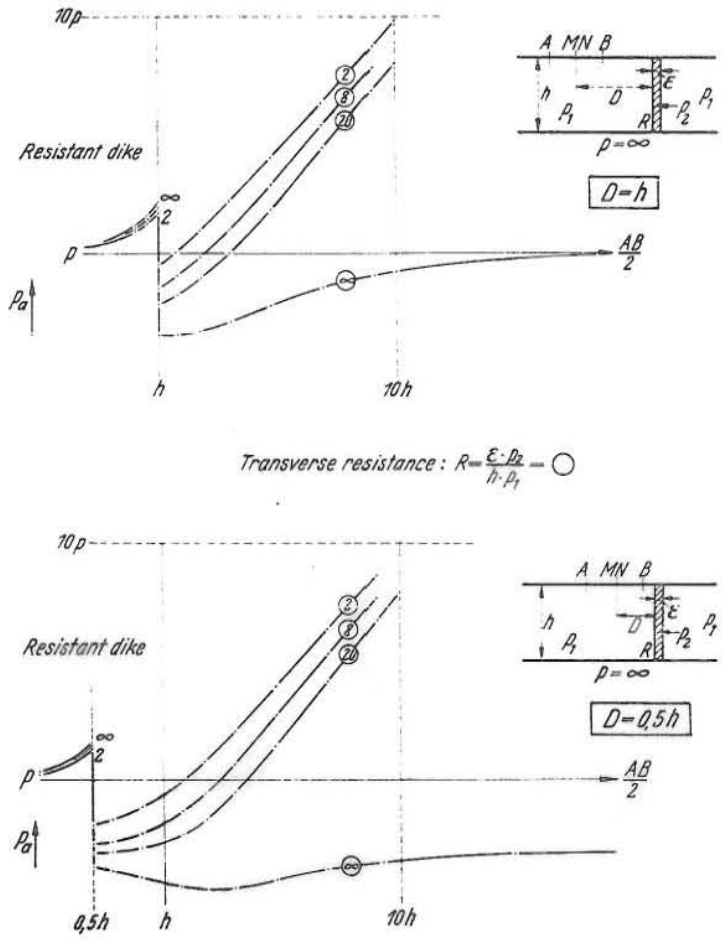

Fig. 2.6 Resistivity soundings near a thin vertical dike underlain by an infinitely resistant substratum (from Kunetz, 1966)

2.5 2-D Modelling of the Schlumberger soundings

The apparent resistivity values at a few specified electrode positions are computed by the program of Dey (1976) over two dimensional earth defined by grid nodes.The program uses the algorithm of finite difference method discussed in detail by Dey and Morrison (1976). Using

Ohm's law the potential ϕ at a point defined by (x,y,z) and conductivity $\sigma(x,y,z)$ due to a current source at a point (x_s, y_s, z_s) are related in the partial differential expression

$$-\bar{\nabla}\cdot[\,\sigma(x,y,z)\bar{\nabla}\phi\,(x,y,z)\,] = \frac{\partial\rho}{\partial t}\delta\cdot(x_s)\delta(y_s)\delta(z_s) \qquad (2.5.1)$$

The layers are assumed to be infinite in the strike direction so that if the conductivity in the y direction is made constant, eq.(2.5.1) becomes

$$-\bar{\nabla}\cdot[\,\sigma\,(x,z)\;\bar{\nabla}\phi\;(x,y,z)\,] = \frac{\partial\rho}{\partial t}\,\delta(x_s)\delta(y_s)\delta(z_s) \qquad (2.5.2)$$

Equation (2.5.2) can easily be solved by taking the Fourier transformation K_y of y. The transformed form of equation (2.5.2) is

$$-\bar{\nabla}\cdot[\,\sigma\,(x,z)\;\bar{\nabla}\tilde{\phi}(x,K_y,z) + k_y^2\,\sigma(x,z)\tilde{\phi}(x,K_y,z) = \tilde{Q}\delta(x_s)\delta(z_s) \qquad (2.5.3)$$

where $\tilde{\phi}(x,K_y,z)$ is the transformed potential equation and $\tilde{Q}$ is the constant steady state current density in the (x,y,z) given by

$$\tilde{Q} = \frac{I}{2\Delta A}$$

ΔA is a representative area in the x-z plane around the current source at (x,y,z).

The solution of $\tilde{\phi}(x,K_y,z)$ in equation (2.5.3) is obtained by the finite difference method by an area discretization

in a grid. The boundary conditions, namely continuity of the potential and the current density across the boundaries, are considered in the formulation of the finite difference equations. The solution is obtained by the approximation of a system of linear finite difference equations in the form

$$\Sigma\ C^{ij}\ (K_y)\ \tilde{\phi}_{ij}\ (K_y) = \frac{I}{2}\ \delta(x_s)\delta(z_s) \qquad (2.5.4)$$

where C^{ij} is the coupling coefficients between nodes. The program of Dey (1976) solves equation (2.5.4) for a given resistivity model and positions of current source points for a certain number of filter values K_y. After a Fourier transformation the values of potential ϕ in the (x,y,z) domain are obtained and used to determine the apparent resistivity.

The rectangular grid used consists of 113 nodes in the x-direction and 16 nodes in the z-direction. At the centre of the sounding, the grid is equally spaced but it becomes more widely spaced farther apart in order to simulate the infinite extent of the model layers. This is also the case in the z-direction. The nodes are defined in unit lengths so that it is possible to change the length of a unit when desired.

The 2-D earth model is divided into blocks according to the grid and the unit size. Thus, the smallest distance which can be used is the unit length. The current and potential electrode positions are also defined. In fact a net input file is made specifing the grid size, the unit length and the position of the electrodes so that they need not be made each time the program is run.

The determination of the apparent resistivity values depends on the number of filter coefficients and the size of the grid. Usually, the more the filter points and the

bigger the grid the more accurately the apparent resistivity can be determined.However, this is on the expense of much more computer time. The program is written to use a maximum of 30 filter points, 161x32 grid and compute apparent resistivity at 20 current electrode spacings for profiles perpendicular to the strike only. However, because of the computer time and accuracy, 113x16 grid, 9 filter coefficients and 9 electrode spacings are used. This takes about 1 computer hour irrespective of the number of blocks in the earth model using the PDP11/34 computer.

As the model is defined using the grid, it is therefore not possible to define accurately some geological shapes like the dipping contacts or round bodies etc. Another disadvantage is that one is restricted by the unit length. This causes some unrealistic thicknesses and lengths to be used.For example,when the unit length of 25m is used the thinest dike will be 25m whereas dikes are normally about 5m.

An example of a typical 2-D model and the computed apparent resistivity values are given in the Appendix I.

2.6 Head-on profiling

2.6.1 Introduction

Profiling is the process of obtaining the lateral resistivity variations. This is accomplished by using a constant current electrode spacing suitably chosen to penetrate to a desired depth.

The combined "head-on" method has been used with success in the Peoples Republic of China to detect faults and dip directions (Cheng, 1980) but the technique is beginning to spread to the rest of the world.

2.6.2 Procedure and apparent resistivity equation

The head-on profiling method uses the normal Schlumberger 4 electrode array and a fifth electrode,C, fixed at infinity (Fig.2.7).

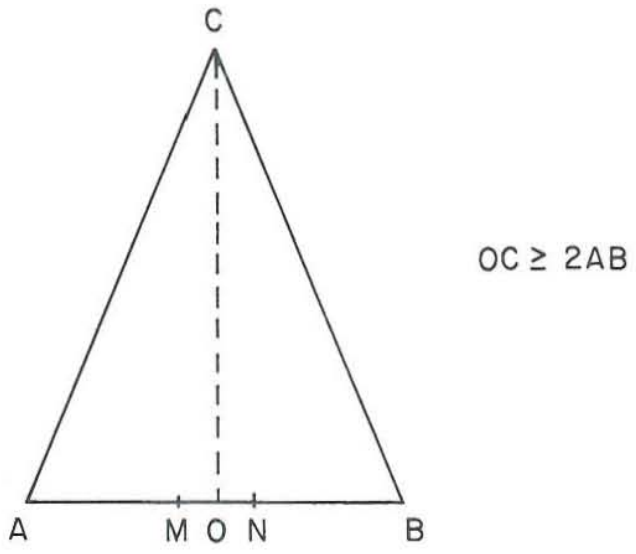

Fig. 2.7 Head-on array

The current is driven into the ground through AC and the potential difference is measured between the usual electrodes, MN. This is repeated with the current through BC and AB. The centre is then moved to the next station along a traverse line.

For a given current I driven between AC or BC, the apparent resistivity is given by

$$\rho_a^{AC} = \frac{\Delta V}{I} \cdot \frac{2\pi}{\left(\frac{1}{AM} - \frac{1}{CM} - \frac{1}{AN} + \frac{1}{CN}\right)} \qquad (2.6.1)$$

Since C is at infinity, 1/CM and 1/CN are approximately zero and equation (2.6.1) becomes

$$\rho_a^{AC} = \frac{\Delta V}{I} \frac{2\pi}{\left(\frac{1}{AM} - \frac{1}{AN}\right)} \qquad (2.6.2)$$

The apparent resistivity is obtained by equation (2.6.2) and it can be shown that the geometric constant is twice that of the Schlumberger array. In fact ρ_a^{AB} is the mean of ρ_a^{AC} and ρ_a^{BC}.

In practice it is difficult to keep C very far. It has been found that it is possible to position C at a finite distance $\geq$ 2AB and determine the resistivity with reasonable accuracy. When using this finite distance, equation (2.6.2) is used to calculate ρ_a^{AC} and ρ_a^{BC}. This demands that the geometrical constant in equation (2.6.1) be determined for each position of the stations. For a station perpendicular to C, equation (2.6.1) reduces to equation (2.6.2). However, for the stations on either side of C the geometric constant differs from that of equation (2.6.2). The error which would be realized if the geometric constant of equation (2.6.2) was used constantly has been computed by the author. The maximum error of

about 2.3% occurs when the station and electrode C are at an angle of about 54 degrees to the profile. The error decreases for greater and lesser angles. This error is in general small and therefore, equation (2.6.2) can be used all the time for the determination of the resistivity.

2.6.3 Head-on profiles over thin dikes

Fig.(2.8) shows the shapes of $\rho_a^{AC} - \rho_a^{AB}$ and $\rho_a^{BC} - \rho_a^{AB}$ across a thin conductive and resistive dikes. These model graphs are computed by a modified version of Dey (1976) program. Since ρ_a^{AB} is the mean of ρ_a^{AC} and ρ_a^{BC}, it has been found convenient to plot $\rho_a^{AC} - \rho_a^{AB}$ and $\rho_a^{BC} - \rho_a^{AB}$. It can be seen from Fig.(2.8) that the graphs of ρ_a^{AC} and ρ_a^{BC} cross each other just above the dikes. The profiles for the conductive dike can be explained as follows: When the centre of the array is to the left and electrode B is to right of the dike, some of the potential due to B is concentrated at the dike so that the potential at the measuring electrodes is less than that due to A. As the measuring centre approaches the dike, the screening effect of the dike is stronger and the potential due to B further decreases whereas that due to A increases. However, when the centre is at the dike, the potential due to A and B is the same. The situation is reversed beyond the dike.For the resistant dike, the graphs cross at three places the middle one being centered at the dike.

The graph of the ρ_a^{AB} for the conductive dike has a characteristic trough whereas a resistant dike has a crest. It is therefore possible to use the head-on crossover as signatures for the exploration for low resistivity dikes and distinguish them from the resistant ones.

Some theoretical head-on models are presented in chapter 4 of this report.

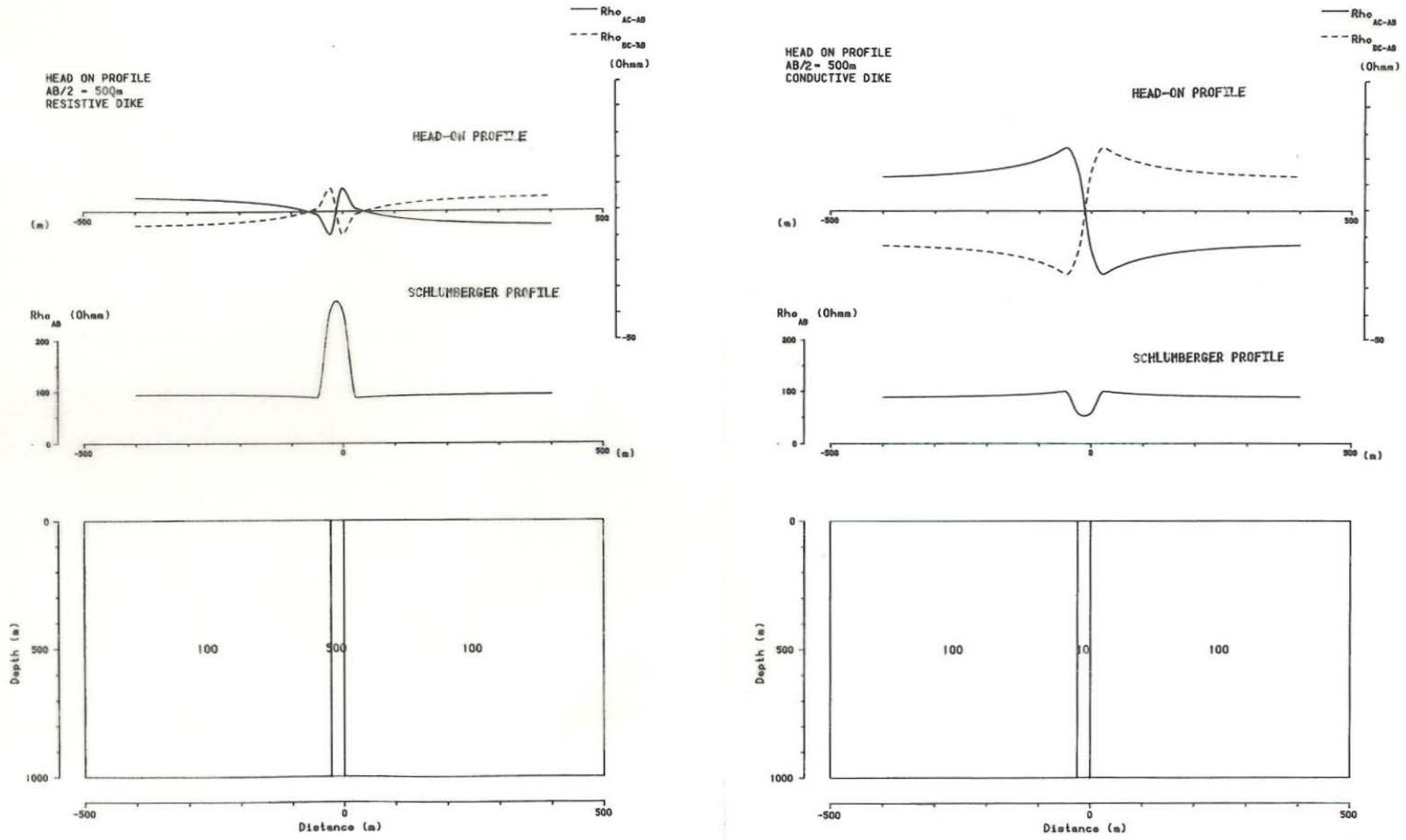

Fig. 2.8 Head-on and Schlumberger apparent resistivity profiles over resistive and conductive dikes

3. 2-D SCHLUMBERGER SOUNDING INTERPRETATION

3.1 Introduction

Geophysical inverstigations have been made in the vicinity of the town of Akureryi in the Eyjafjörður area in central northern Iceland. Resistivity soundings and magnetic measurements have been used to locate drill holes close to the town. Six successful wells 12km south of Akureyri produce about 150 l/s of 80-96 °C hot water (Bjornsson,1981).

Eyjafjordur is a V-shaped valley and most of the earlier resistivity measurements were made parallel to the valley in order to avoid the steep terrain on the flanks of the valley. The interpretation of the measurements showed that the bottom of the valley contained low resistivity sediments, which made the 1-D interpretation of the resistivity sounding data difficult. In 1981, measurements were carried out perpendicular to the valley so that they could be interpreted by the 2-D modelling techinique (Flovenz and Eyjolfsson, 1981).

Some of these recent soundings have been reinterpreted by the author as a training excercise in the 2-D modelling method of the Shlumberger data.

3.2 Geological setting

The strata around Akureyri consists of Tertiary subaerial basaltic lava flows 8-10 M.y. old. The individual lava flows are thin and are occasionally intercalated with sediments and volcanic scoria. The lava pile dips by 5-7 degrees south and southeast towards the Neovolcanic zone. Dikes are numerous and form about 6% of the total volcanic mass (Bjornsson and Saemundsson, 1975). The main faults have the same direction as the dikes.

Prior to drilling there were about 20 locations with hot springs with an initial natural flow of about 14 l/s. The temperature of the springs ranged from 10 to 70 °C.
These springs are associated with dikes and occur particulary where two dikes intersect. Therefore, apart from detecting the general hot water areas commonly characterized by low resistivity due to high porosity, the geophysical investigations have been aimed at mapping the dikes associated with hot water which are usually buried under an overburden and therefore, difficult to map geologically.

3.3 Resistivity measurements

A total of 120 Schlumberger soundings were made between 1975 and 1980 and 35 more soundings in 1981 (Fig.3.1). The latter soundings were measured perpendicular to the Eyjafjordur valley specifically for the 2-D interpretation around Laugaland and Gryta. Most of these recent measurements were expanded to a maximum electrode spacing of AB/2=1580m and the sounding locations were so chosen that the neighbouring current electrode spacings overlapped. The overlap is very important because it helps to identify and locate the strong lateral resistivity variations which might be confused for bad measurements etc. The 1981 soundings were of high quality even at large current electrode spacings because they were measured with dc-equipment which employs a modern signal enhancement receiver. Therefore, most of the jumps or breaks in the apparent resistivity curves can be attributed to vertical boundaries and surface inhomogeneities.

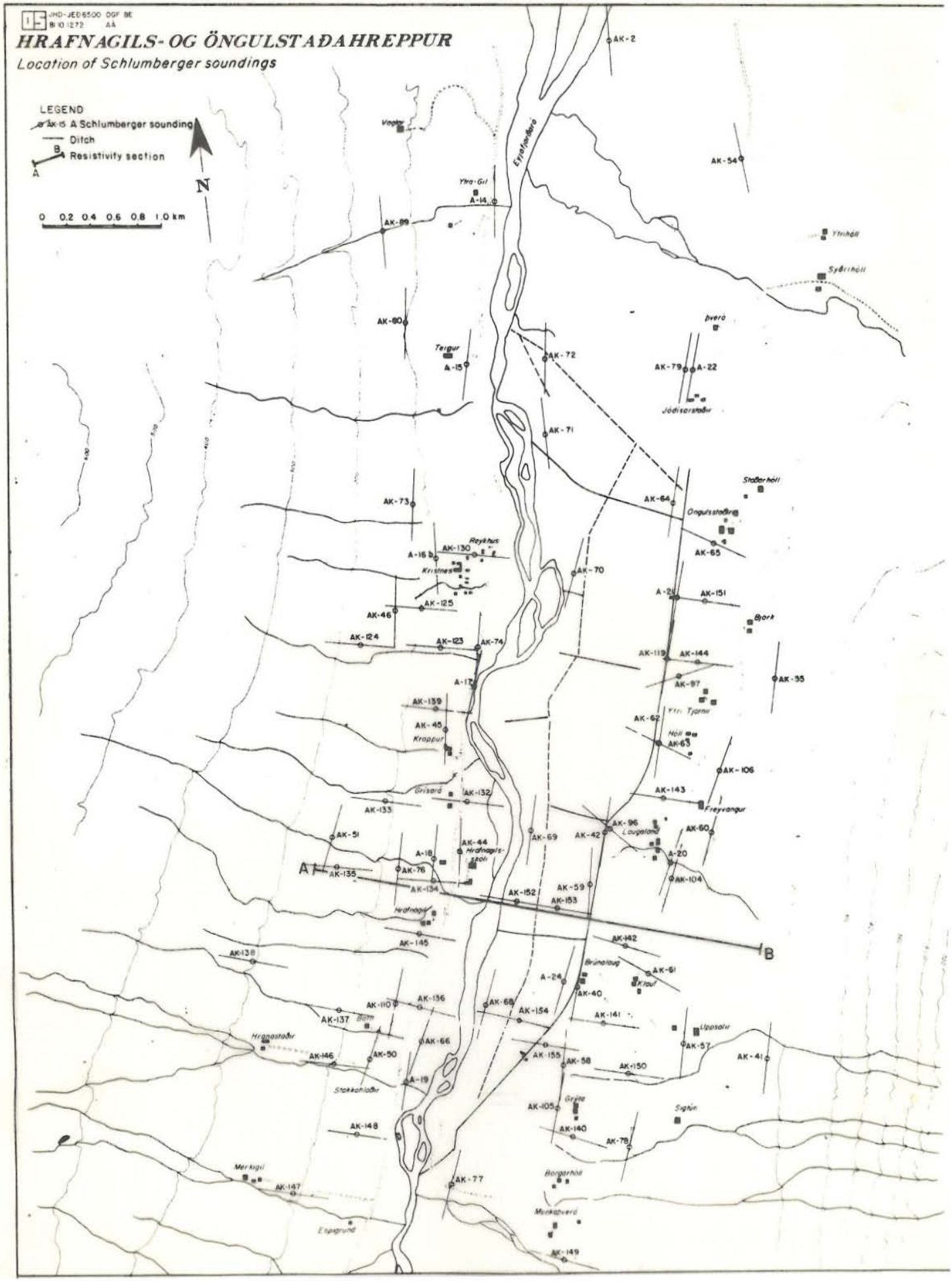

Fig. 3.1 Map of Eyjafjördur showing the location of Schlumberger soundings and interpreted resistivity profile (Flovenz and Eyjolfsson, 1981).

3.4 The 2-D Interpretation

3.4.1 Initial model approximation

A Schlumberger sounding made over non-horizontally layered earth is characterized by sharp bends or breaks or steeply rising branches often exceeding the maximum 45 degrees slope as mentioned in chapter 2. If the 1-D interpretation is used, the results can be quite inaccurate. To illustrate this sounding AK69 from Eyjafjordur (Fig.3.2a) is considered. At a glance, the slope between AB/2=250m and 900m is about 55 degrees. The data was fitted by an automatic iteration program CIRCLE2 without applying any constrains. Using a 5-layer model, the fit in the last part of the curve is poor, the resistivity of the fourth layer too low and that of the fifth layer obviously too high and its depth too shallow. It can then be concluded that the sounding is affected by a vertical boundary between a low resistivity layer, say, < 10 ohmm and a much higher resistivity layer. However, some unaffected parts of the curve can be interpreted one dimensionally. The last part of the curve beyond AB/2=250m was ignored and the rest computed by CIRCLE2 program. The results are given in Fig. (3.2b). It can be seen that the part of the curve beyond AB/2=900m has a constant slope of 40 degrees. This slope depends on the resistivity contrast between the low resistivity and the underlaying layer. The effect of the resistivity contrast at the vertical boundary shifts the curve vertically for resistivity ratios of up to about 9. However, very little changes occur for ratios above this (See Fig.2.5).

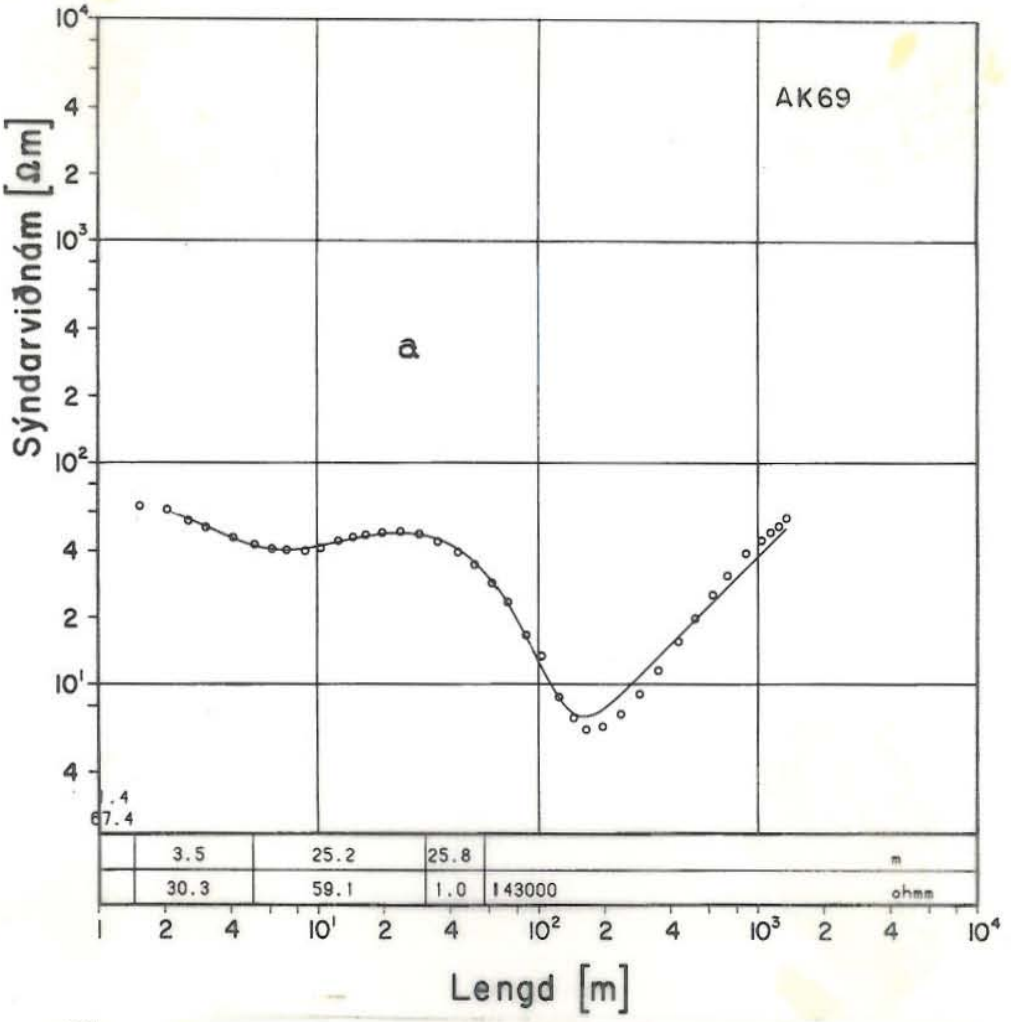

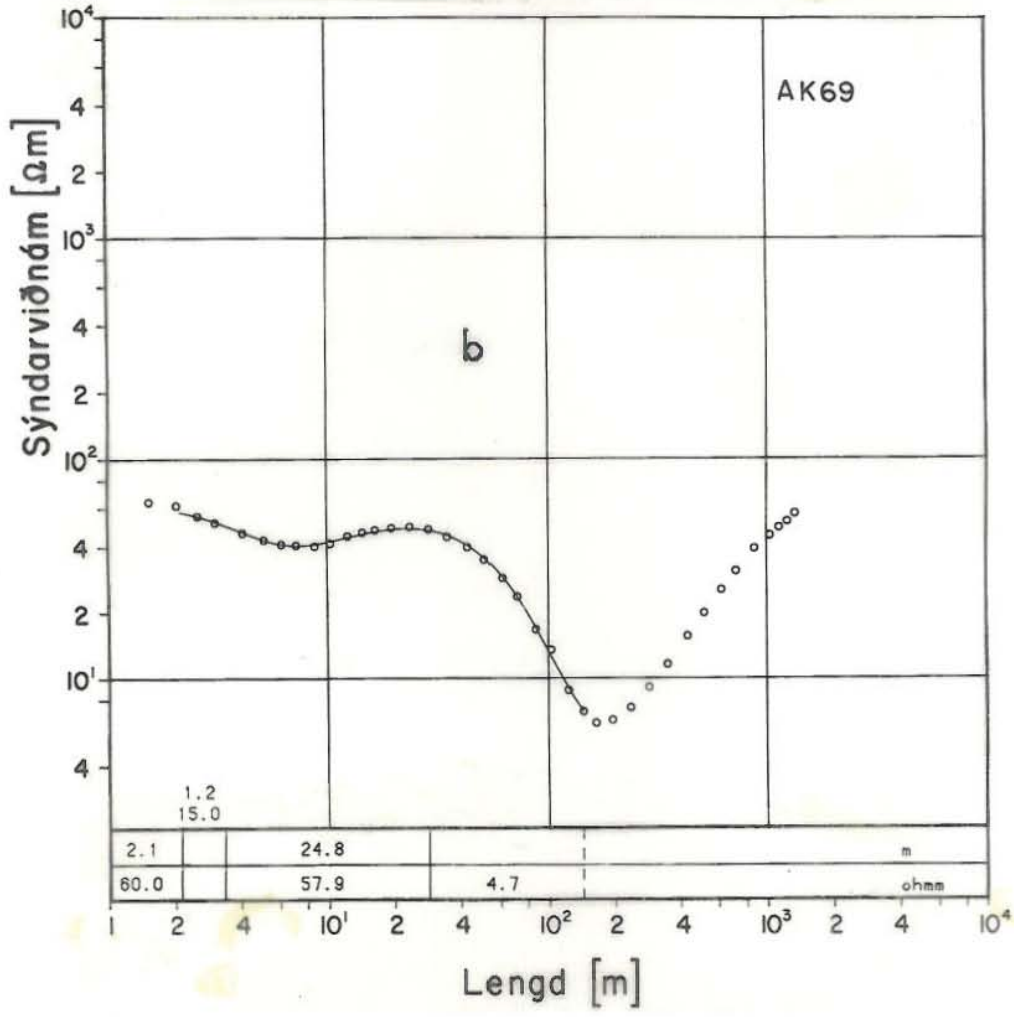

Fig. 3.2 CIRCLE2 fits to AK69 sounding curve.

If we assume a ratio of at least 9, and the resistivity of the low resistivity layer to be 5 ohmm from CIRCLE2, then the resistivity of the medium beyond the contact is at least 45 ohmm or more. The resistivity of the substratum is at least 200 ohmm if it is assummed the resisitivity contrast causing the 40 degrees slope is about 40.

The vertical shift of the curve due to the substratum is smaller than that caused by the position of the vertical contact. As the distance to the contact is increased the effect is delayed. This is because the vertical boundary affects the potential horizontal current flow pattern before the current penetrates too deep into the underlaying layers. The low resistivity layers have a strong effect and cause sharp V-shapes in the curve. For the high resistivity boundary of AK69, the position of the contact is at the value of AB/2, where the steep slope join the 40 degrees part of the last branch. This happens at AB/2=800m.

Using CIRCLE2 program, five E-W Shlumberger soundings from Eyjafjördur were interpreted and the fitted curves are shown in Appendix II. The procedure mentioned above was used to infer the main vertical boundaries.

The shallow thin layers and inhomogeneities were ignored. However,layers thicker than 25m in the first 100m depth were considered. Actually, the average resistivity for the first 25m was used in the model. The procedure discussed above was used to infer the vertical discontinuities, considering all the neighbouring soundings. The interpreted section is shown in Fig.(3.3).

The interpretation started from sounding AK152 on the valley floor. The sounding is located on a low resistivity area whose resistivity was estimated to be about 5 ohmm.

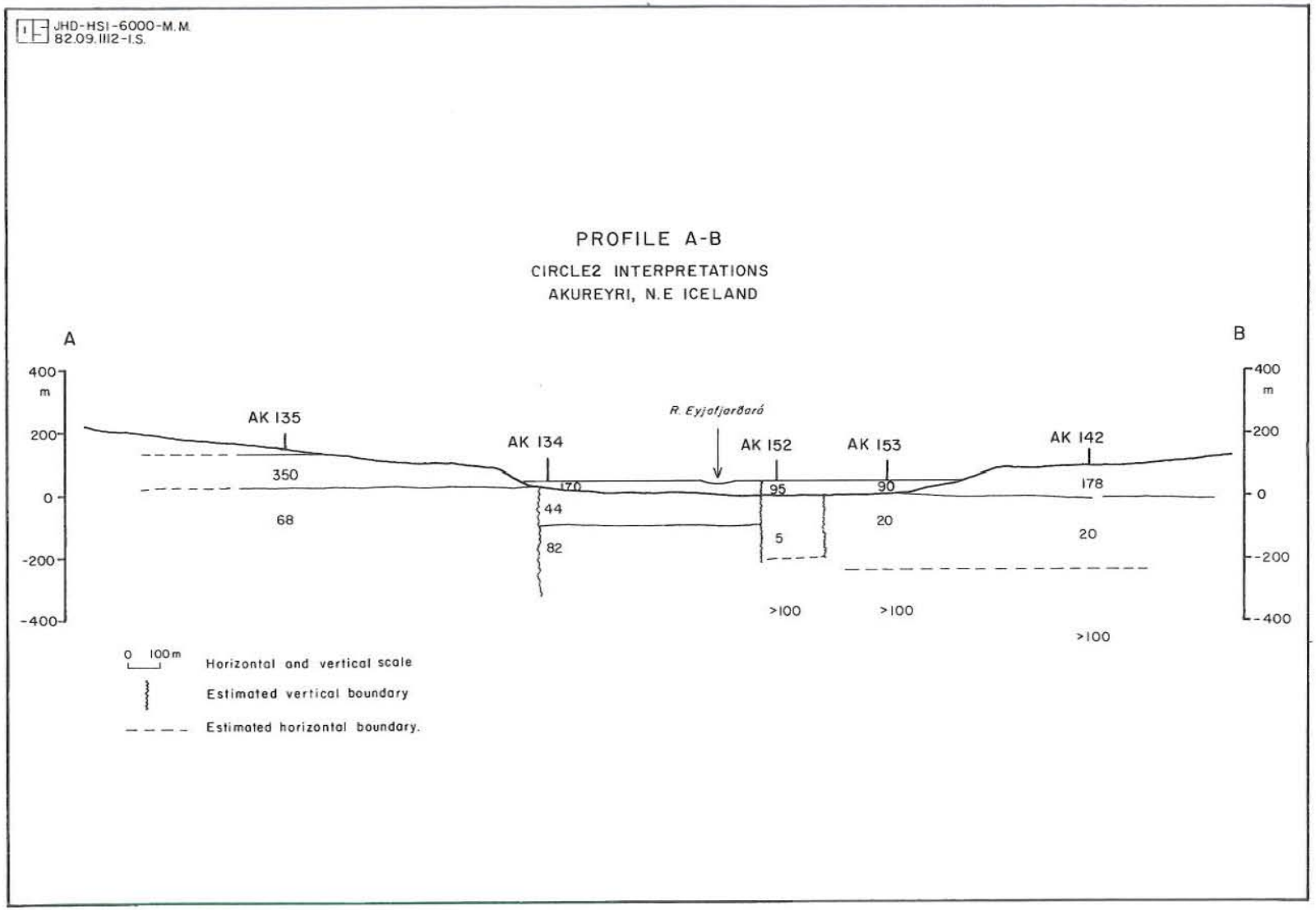

Fig. 3.3 CIRCLE2 interpretation section of profile AB

The steeply ascending last branch of the curve indicates that there is a much higher resistivity change either vertically or laterally or a combination of both. This sounding is short but it seems to have a general shape as AK69 which is located 600m to the north and expanded along the strike of the valley. The vertical contact as interpreted from AK69 is 800m to the north. The sounding also reveales a high resistivity substratum with a value of about 200 ohmm. It is assumed that the substratum at AK152 probably has a resistivity of the same order of magnitude.

Sounding AK153 differs slightly from AK152 and it shows an elevated resistivity layer (20 ohmm) overlying the substratum. A sharp minimum at AB/2=250m marks the boundary between the 5 ohmm and the 20 ohmm layers on the AK152 side. The slope of the last part of the curve is steep but less than 45 degrees. The interpreted resistivity of 200 ohmm is either true or overestimated because of a vertical boundary. Again the sounding was too short to be used further.

The 20 ohmm layer found at AK153 is confirmed by AK142. The interpreted resistivity of the substratum by CIRCLE2 is about 400 ohmm. Noting that the interpreted depth to the substratum is about the same both from AK153 and this sounding, it would appear that the difference in the interpreted substratum resistivity is attributable to the presence of a probable vertical contact which is not apparent from both these curves. There is no sounding much further to the east of AK142 which could be used to decide this side of the boundary.

However, considering AK134, a thick resistivity layer of about 80 ohmm is seen and it could extend laterally towards AK152. The sharp minimum at AB/2=850m marks the western boundary of the low resistivity of 5 ohmm. The 80 ohmm layer extends eastwards and it is the one affecting soundings AK152, AK153 and AK142. The reason why the boundary can not be clearly identified from AK152 is

because the minimum of the curve, due to the substratum, coincides with the contact. Sounding AK135 is interpreted reasonably well except that the last branch indicates a high resistivity vertical contact at 1300m to the west of the sounding. This is because the contact can not be correlated with any other on the eastern side.

3.4.2 2-D computer modelling

In the 2-D modelling, as mentioned in chapter 2, the earth medium is divided into blocks of thicknesses and lengths in a multiple of a specified unit length. The Shlumberger apparent resistivity at various electrode spacings is computed and the curve compared with the measured one manually. The resistivity and the block sizes are changed until a reasonable fit is obtained.

The section interpreted one dimensionally was used as the initial model. The boundaries were arranged according to the grid of a unit length 25m. For each sounding, the model was defined at least over a distance greater than 1500m which was about the maximum electrode spacing used in the field measurements. This ensured that the relevant information over 80% of the profile was included. The results of the 2-D modelling is given in Fig.(3.4). The apparent resistivity pseudosections of the computed and measured curves are shown in Fig.(3.5).

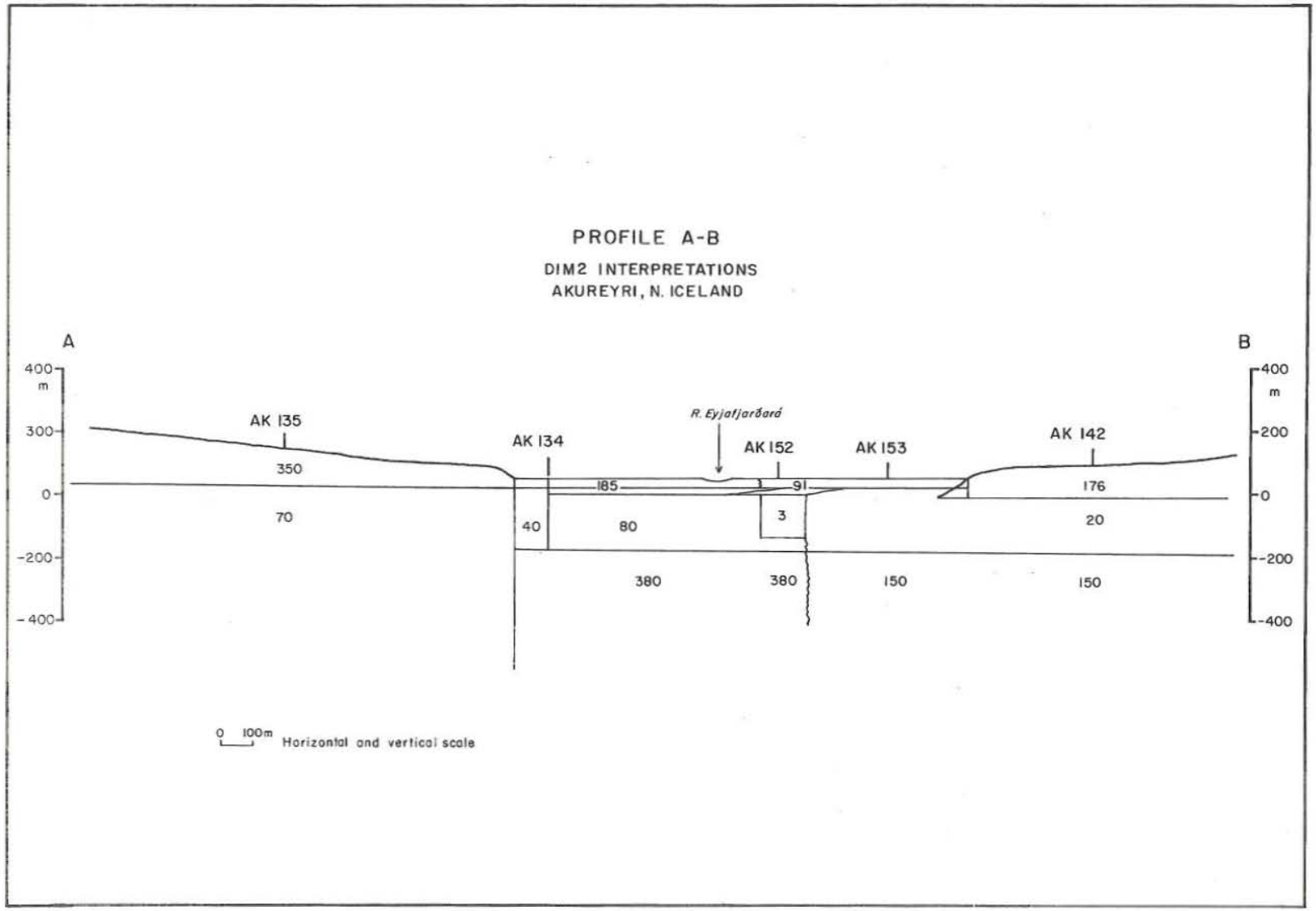

Fig. 3.4 2-D interpetation section of profile AB

MEASURED APPARENT RESISTIVITY PSEUDOSECTION

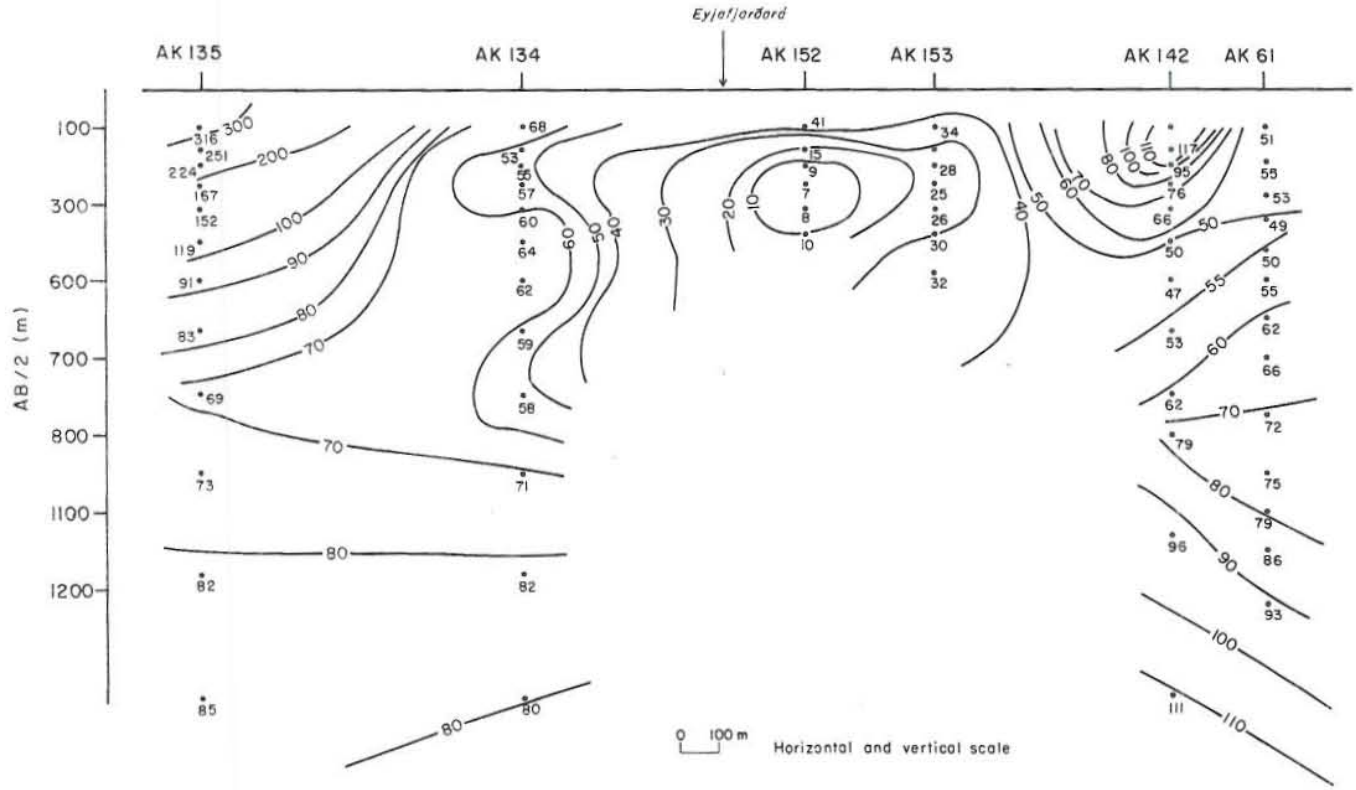

COMPUTED APPARENT RESISTIVITY PSEUDOSECTION

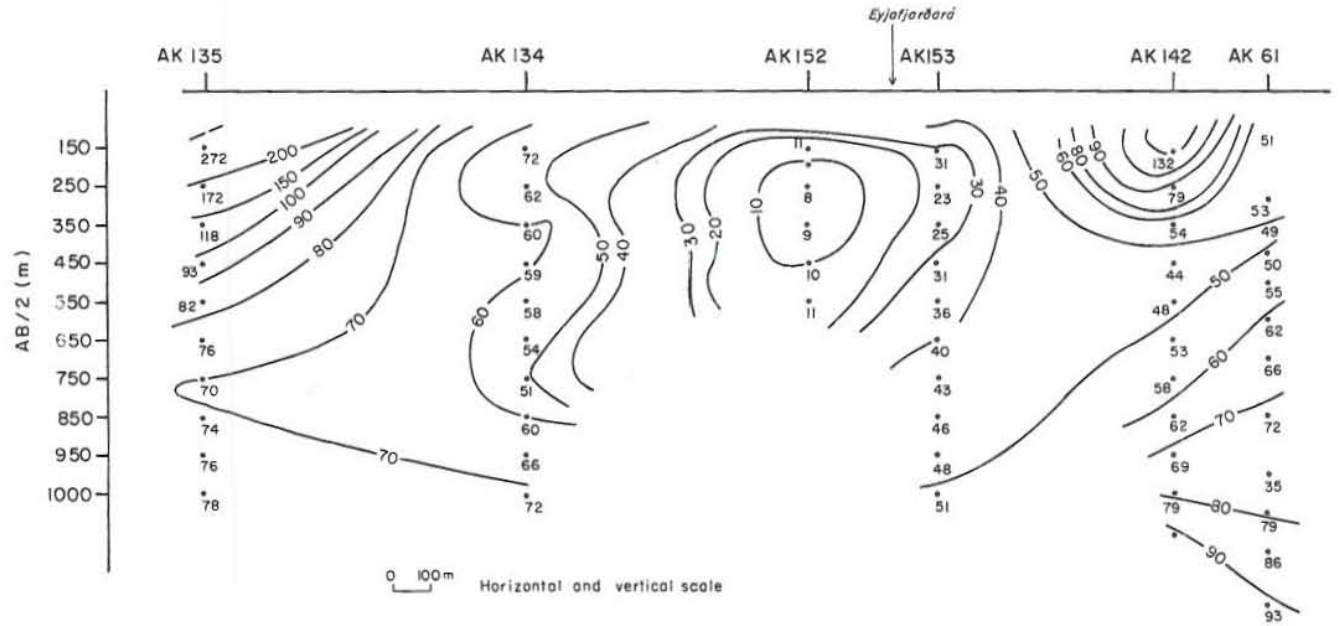

Fig. 3.5 Measured and computed pseudosections.

3.4.3 Results of the modelling

The pseudosection of the computed apparent resistivity agrees very well with that of the field data. These, together with the computed model, seem to reflect the geophysical condition of this area. The most important features affecting the model are the low resistivity of about 3 ohmm at AK152, the vertical contact immediately to the west of AK152, and the resistant substratum. Sounding AK134 was the most difficult to fit into the profile (Fig.3.4). The 40 ohmm block just below AK134 was found necessary to be included in the profile. It seems not to extend to the west because it would affect AK135 badly. If the simple model was to be maintained, the 380 ohmm substratum below AK134 and AK152 had to be used.Decreasing this resistivity produced a poor fit. Yet, it could not be extended to AK153 and AK142. Keeping the model constant, resistivities much higher than 150 ohmm again affected the fits of AK153 and AK142. The only way of reducing the resistivity of the substratum below AK134 to AK142 was by inserting blocks of high resistivity in the upper 200m, an exercise that would make the whole model not only too complicated but also cause uneven depth to the substratum difficult to explain. Not all the resistivities could be tried between 200 ohmm and 400 ohmm but the resistivity is in this range. There is a vertical contact about 1200m to the west of AK135 not shown in the section. This was necessary to account for the ascending last branch of this sounding.The high resistivity substratum seems to be absent at AK135. Any attempt to include this substratum demanded the presence of a low resistivity block, say of about 40 ohmm, below the sounding. The effect of this block caused most of the curve for AB/2 < 850m to fit badly unless more changes were made to the overlying 350 ohmm layer which is consistent in the neighbourhood. Sounding AK51 located close to AK135 (see Fig.3.1) indicate rather clearly that, the layer below 350 ohmm layer is too thick as the interpretation of AK135 shows.

Compared with the 1-D interpretation, the 2-D model is nearly the same. The major differences are the presence of the 40 ohmm block at AK134. The 2-D model defines the depth to and the resistivity values of the substratum. The resistivities are in a reasonable order of magnitude, the differences being attributable to equivalence caused by the use of a fixed grid in the 2-D program.

The resistivity of the conductive sediments in the valley is in the range of 3-5 ohmm and their base is not more than 200m below the surface or about 125m below sea level. The 2-D model also shows the discontniuty of the substratum west of AK134 and its decrease in resistivity to the east of AK152. The 1981 model of Flovenz and Eyjolfsson (1981) is presented in Fig.(3.6). Comparing this and the present

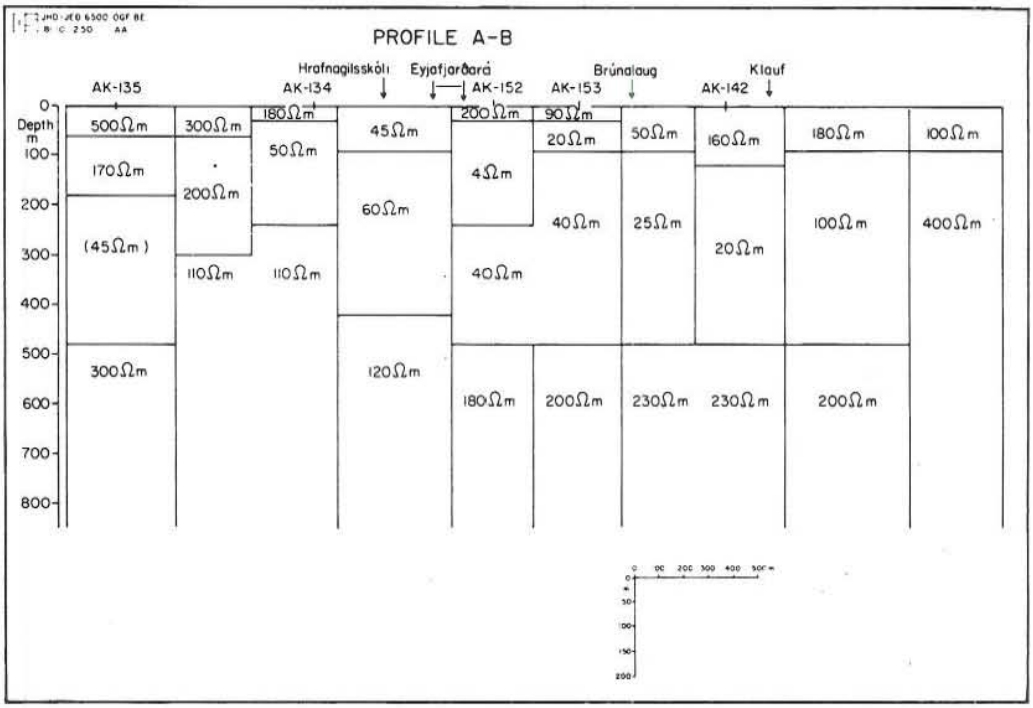

Fig. 3.6 Two dimensional model made in 1981, (Flovenz and Eyjolfsson, 1981).

model (see Fig.3.5), they both reflect the same overall resistivity in the Eyjafjördur area near Laugaland.The main difference is that the present model is much simpler and seems to define the top of the resistive substratum more clearly.

3.5 Discussion

In the 2-D modelling, the problem of equivalence is common. The reasons for this are mainly due to the grid inflexibility in the 2-D program on the one hand, and the infinity set of solutions inherent in the resistivity method on the other. One way of reducing the problem is by constraining the model using some information from drilling, geophysical logs etc. Since this external information was lacking, the problem of equivalence must not be overlooked. However, the models indicate the main geophysical boundaries which are extremely useful.

The main structures to be inferred from the present work are:

(1) The conductive 3-5 ohmm sediments in the middle of the Eyjafjörður valley, which are of marine origin deposited after the formation of the fjord. The base of these sediments mark the bottom of the glacial valley which is about 200m below the surface.

(2) A decrease in resistivity east of the valley.

(3) A discontinuity immediately to the west of AK134 which could probably be a fault.

It is uncertain wether the 20 ohmm layer is associated with the hot water. According to Flovenz and Eyjolfsson (1981), the decrease in resistivity in the low-temperature area is a function of porosity. It would seem therefore, that the rocks in the eastern side of the valley are

probably more permiable. Bjornsson (1981) and Flovenz and Eyjolfsson (1981) are of the opinion that the hot water in the Eyjafjörður area flows along the dikes and appears as springs at various places. Soundings AK140, AK153, and AK155 (Fig.3.1) to the south of the profile, indicate the presence of a north-south dike but none of the soundings in this profile.

3.6 Conclusions

The present work clearly demonstrates how the 1-D and 2-D methods can be intergrated to improve the Schlumberger sounding interpretations.

A simple model was favoured; the more complicated the model was made the more difficult and frustrating the modelling became. It was actually found worthy to recognize the distorted parts of the Sclumberger soundings carefully to mark the consistent vertical boundaries, and to use all the available data from the area. The 1-D interpretation should be used as far as possible to control the 2-D modelling.

The sediments in the middle of the Eyjafjörður valley are not extensive laterally and their base does not exceed 200m below the surface. The sediments overly a resistant substratum with a resistivity of 100-400 ohmm. The hot water implication is not clear from the model. It is therefore agreed that the main conduit of the hot water appearing as springs at Laugaland and elsewhere is probably assosciated with dikes. Dikes, unless they are more resistive than the surrounding rocks, would be rather difficult to detect by Shlumberger soundings so that other methods,for example magnetic and head-on, have to be resorted to.

4 HEAD-ON THEORETICAL MODELS

4.1 Introduction

The apparent resistivity profiles for the head-on configuration (Fig.2.7) were computed using a 2-D finite difference program, DIM2K, over several simple 2-dimensional structures. It is convenient to plot the difference between the head-on and the Schlumberger resistivity values instead of the actual head-on values. The Schlumberger profile is also plotted. The theory of the head-on profile is given in Chapter 2 and the theoretical models are given below. Since the theoretical computation takes a very long time, only a few models were computed. However, the few models will illustrate a few facts about the method and may be found useful in the interpretation of the head-on data.

4.2 Conductive fractures

This is perhaps the most attractive structure as far as geothermal exploration is concerned. It is assumed that a geothermal brine in a fault or a fracture creates a conductive zone. The head-on response over such a zone (hereafter referred to as conductive dike) in a homogeneous earth is shown in Fig.(2.8). The apparent resistivity due to the leading current electrode is less than that due to the lagging one. However, the resistivities are the same over the middle of the dike and the situation is the reverse as soon as the measuring centre crosses the structure. On the other hand, the Schlumberger profile has a trough over the dike. The head-on profiles are symmetrical and the amplitudes decreases gently away from the crossover. The size of the amplitude depends on the resistivity contrast between the dike and the surrounding rock.

4.3 Penetration depth

Fig.(4.1) shows that theoretically, the penetration is up to about AB/2 used in the profiling but the amplitudes are reduced so much that would be difficult to measure it in the field. The measurable data can only be obtained reasonably to a depth of about AB/4. However, if there are strong lateral contrasts in the top layers, the penetration is reduced considerably as shown in Fig.(4.2).

4.4 Inhomogeneities

The head-on data is sensitive to vertical structures very near or on the surface for short electrode spacings. Conseqently, the presence of a crossover may not necessary mean that the conductor extends very deep. Any vertical conductor within the probing depth may cause a crossover provided its size and the resistivity contrast with the surrounding rocks is reasonable. Some examples of models of this type are shown in Fig.(4.3). The Schlumberger profiles show strong electrode effects caused when the electrodes cross the lateral boundaries. Fig.(4.4) illustrates this for the Schlumberger profile with AB/2=300m, which has two lows 300m on either side of the low resistivity structure. These lows may be confused with the resistivity material in the ground; they are absent for AB/2=500m profile. Therefore,during exploration, it is recommended to use larger electrode spacings or to be careful when using the Schlumberger profile in the interpretation. It is most recommended to use two or more electrode spacings so as to prove whether the anomaly still exits to a substantial depth as would be required for a dike.

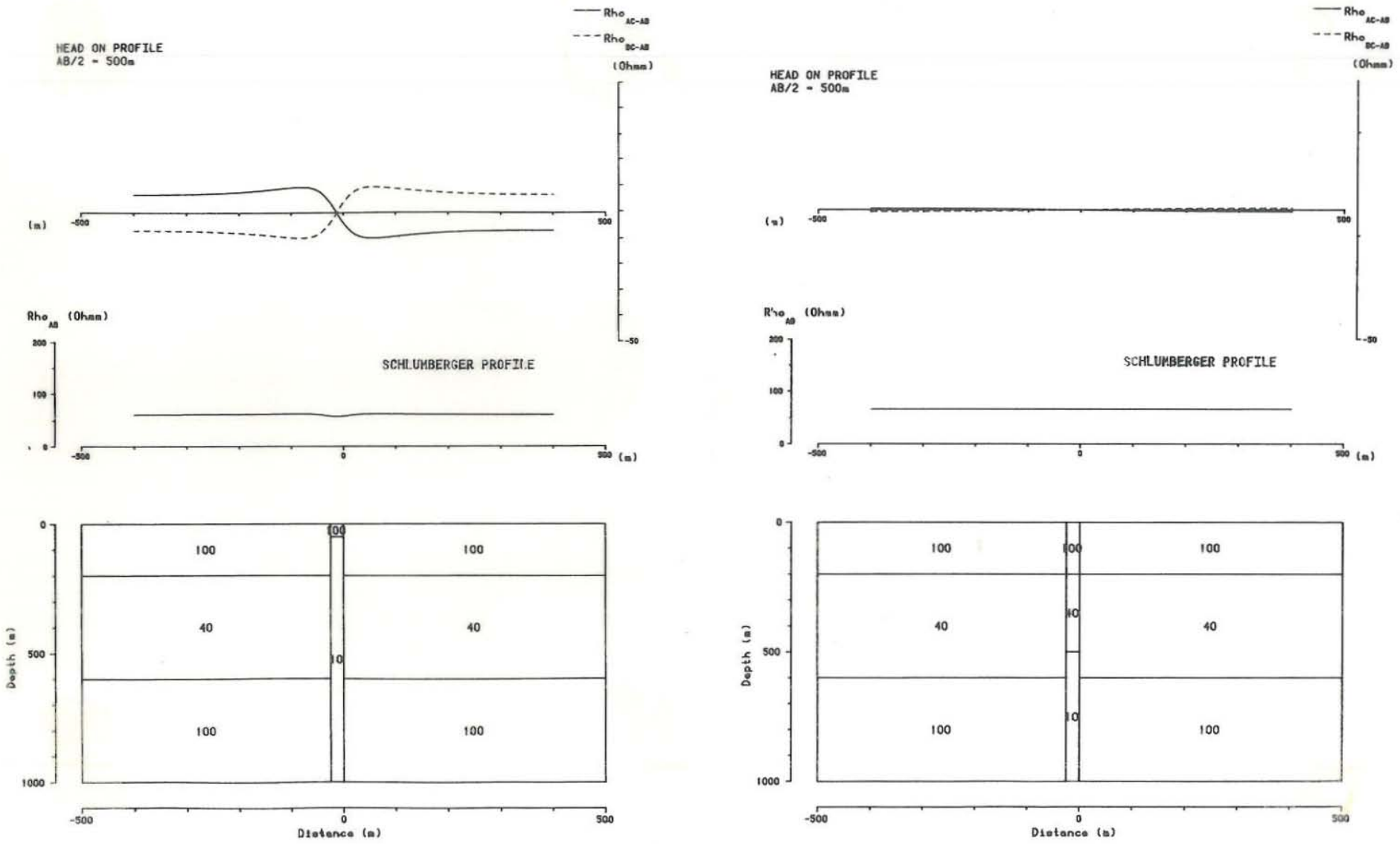

Fig. 4.1 Head-on and Schlumberger profiles over a conductive dike buried at different depths

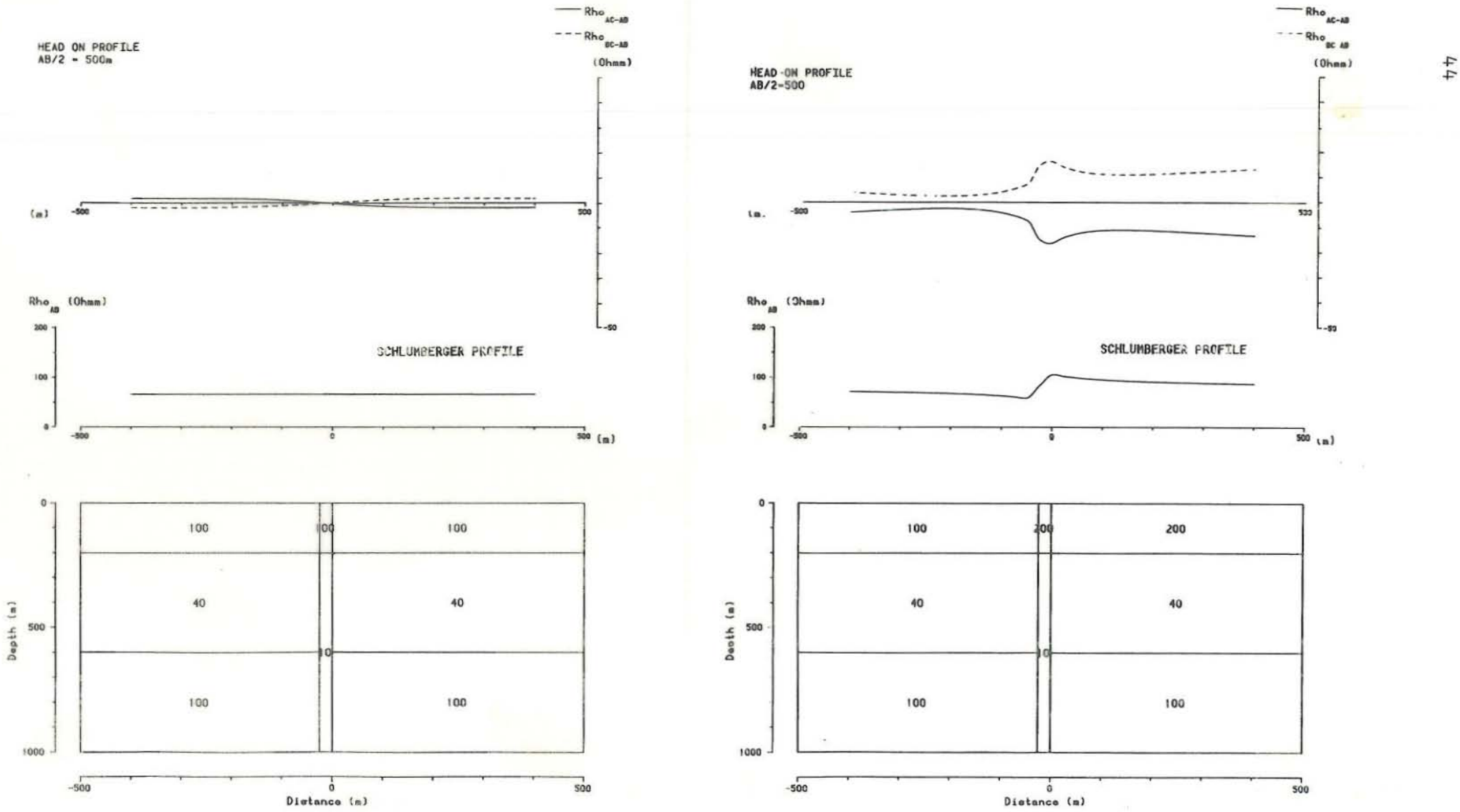

Fig. 4.2 Head-on and Schlumberger profiles showing how the lateral resistivity changes near the surface reduce the penetration depth

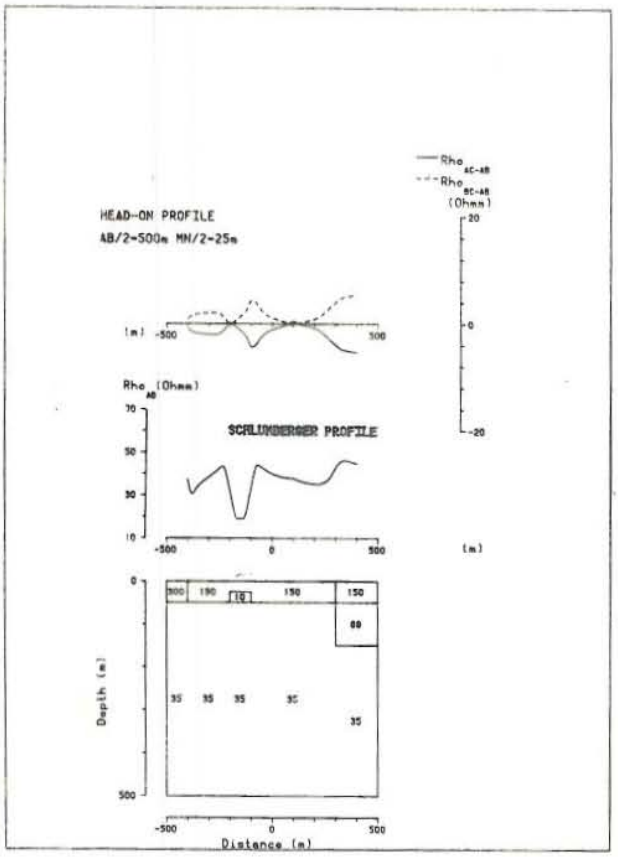

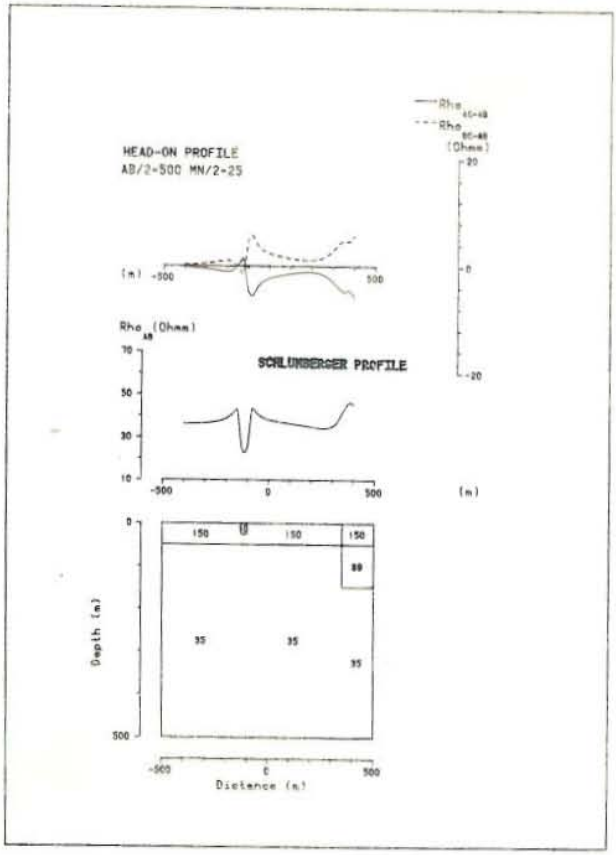

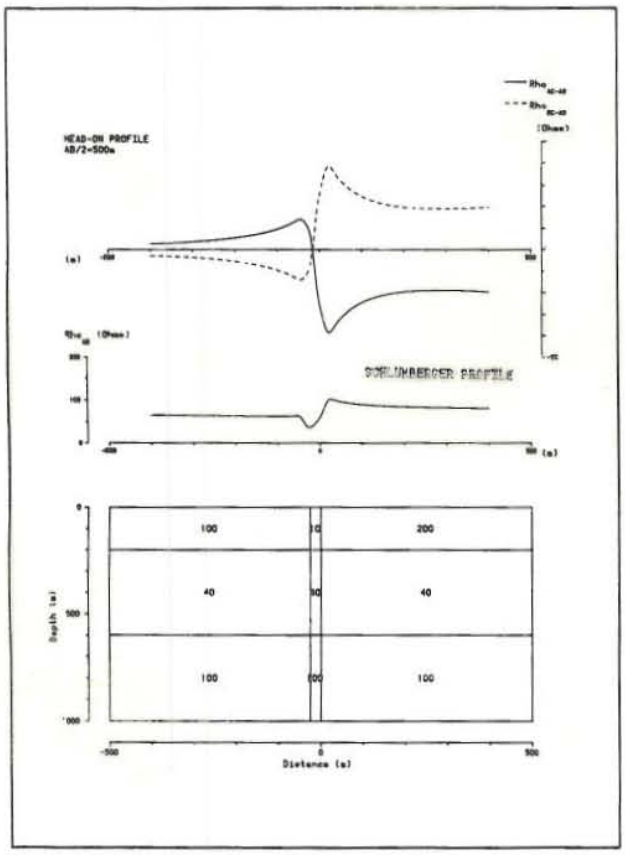

Fig. 4.3 Head-on and Schlumberger profiles over near-surface inhomogenities

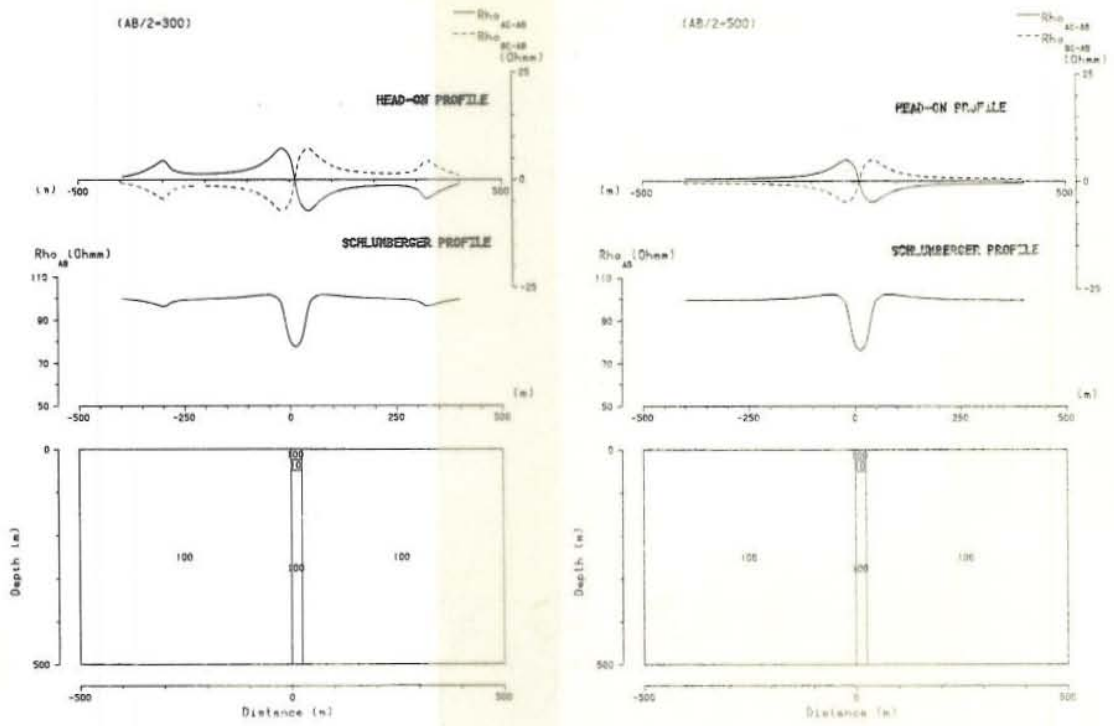

Fig. 4.4 Head-on and Schlumberger profiles showing electrode effects for AB/2 = 300m

4.5 Two conductive dikes or fractures

Two conductive dikes can have a neutralising effect if they are spaced less or equal to the electrode spacing used in the profile measurement. This is more so when the contrast is the same on either side of the two dikes. An example of this case is shown in Fig.(4.5). Note in the figure that the dike to the right causes a crossover but not what would be called a total crossover as would be effected by a single dike. Although the Schlumberger profile has a trough coinciding with the crossover, this is not always the case where the conductive dike is buried by an

overburden and the ground is complicated. Fig.(4.6) shows an example where a resistivity trough does not coincide with the crossover.

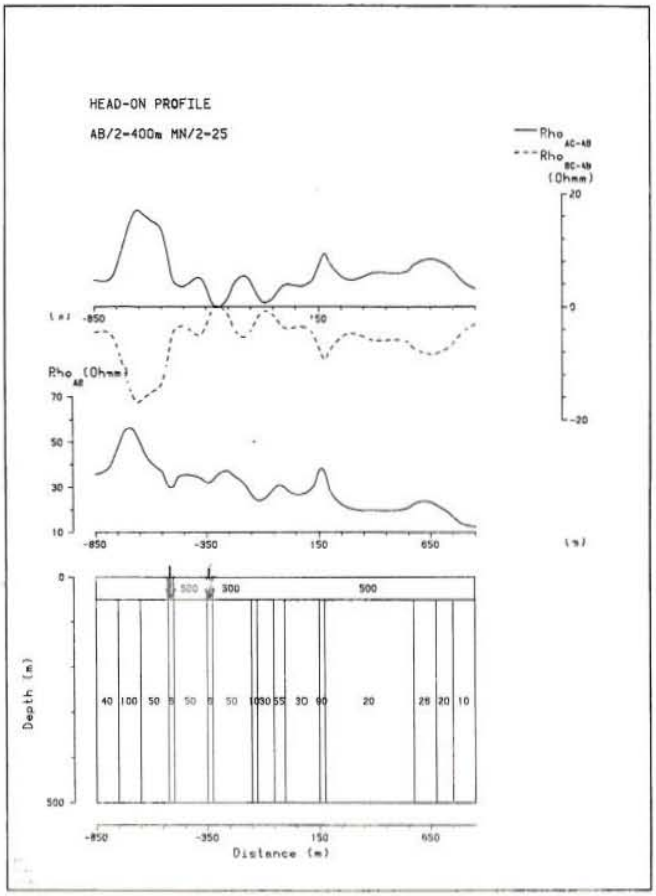

Fig 4.5 Head-on (top) and Schlumberger (center) profiles across two conductive dikes

4.5 Dipping structure

Fig.(4.7) shows the computed head-on profiles over a 45 degrees dipping conductive dike using two electrode spacings. Ideally, the profile with a greater probing detpth is shifted to the direction of the dip. The

Schlumbeger curve also indicates the dip direction. However, owing to usual errors in field measurements over a real earth, the shift is too small and even much less for higher dip angles. The main reason why the shift in the crossover is small with the increase in the electrode spacing is because most of the effect comes from the top part of the dike.

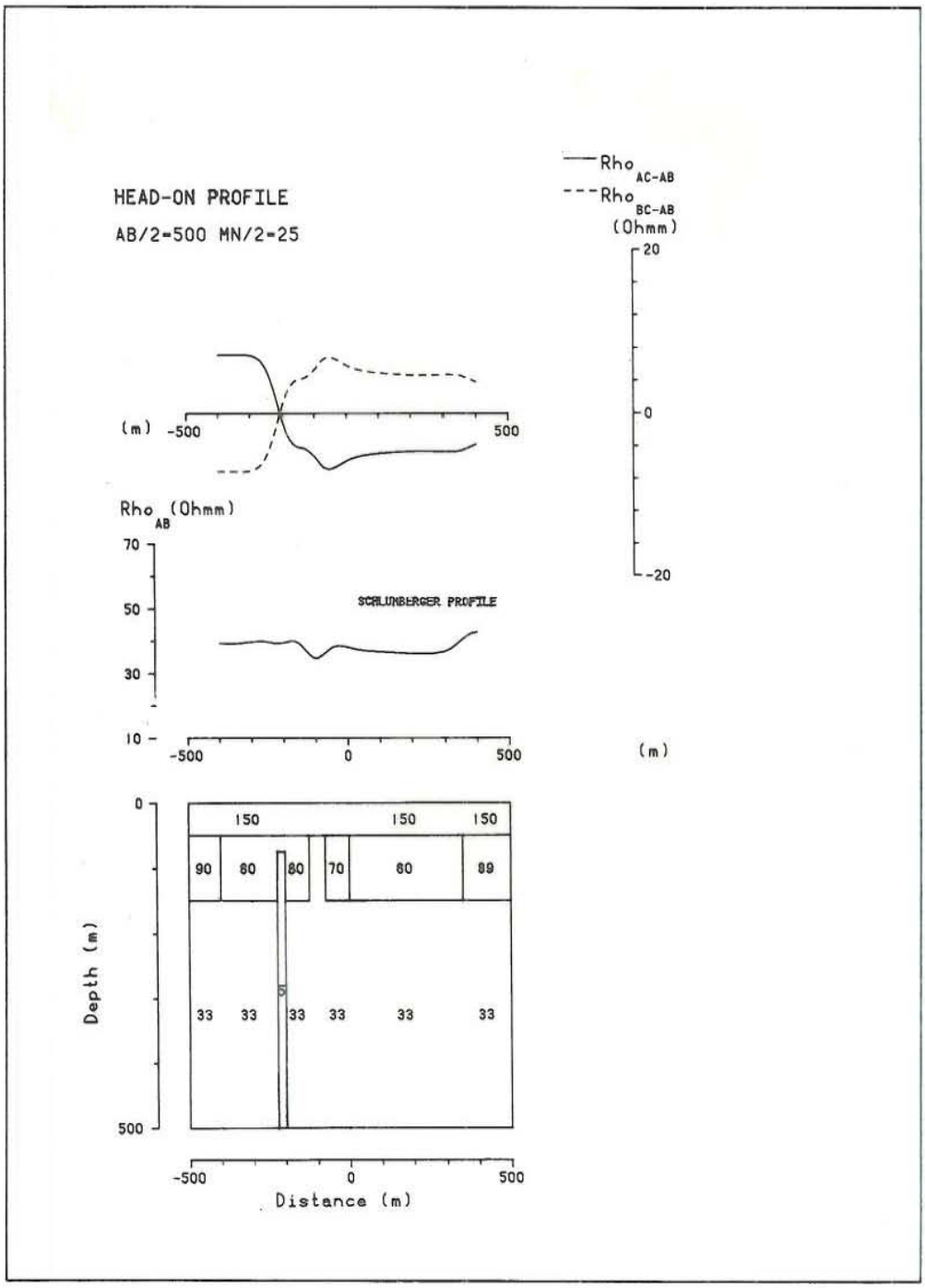

Fig. 4.6 Model whose crossover does not coincide with Schlumberger resistivity profile trough.

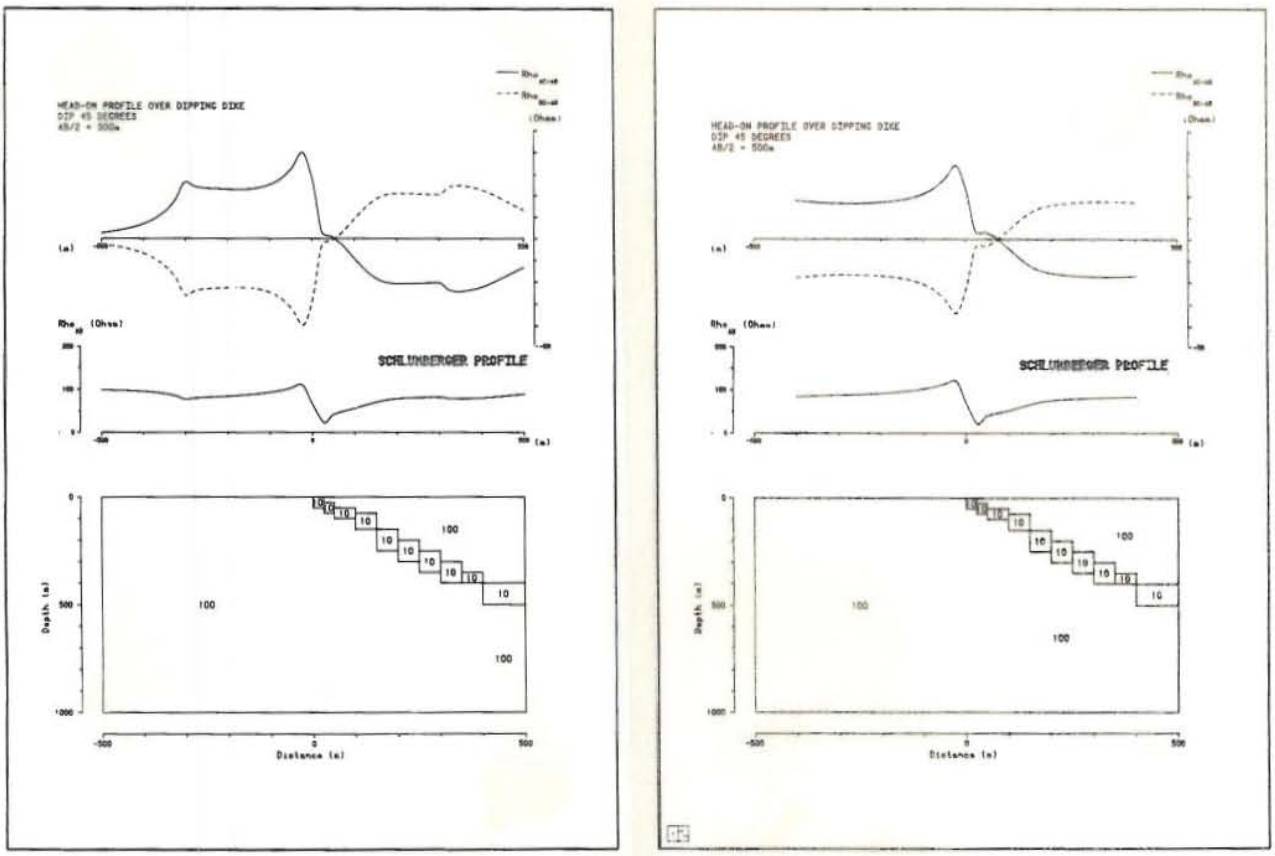

Fig. 4.7 Head-on and Schlumberger profiles over a dipping dike

4.6 Resistive dike

The model profiles for a resistive dike are shown in Fig.(2.8). The dike has three crossovers the middle one being centered over the dike. The profile amplitudes are relatively smaller than those of a conductive dike. As would be expected, the Schlumberger profile has a crest over the dike.

4.7 Vertical contact

The head-on profiles diverge at the vertical contact as shown in Fig.(4.8) and define the contact unambiguosly. It can be gleaned from the figure that it is also possible to know which side of the contact the resisitivity is lower than the other. The Schlumberger profile can be used to approximate these resisitivities. Seemingly, the head-on method can be used to detect structures such as grabens, hosts etc which are very important structures in geothermal fields. Therefore, it is clear that only a narrow structure with a contrasting resistivity would cause a crossover.

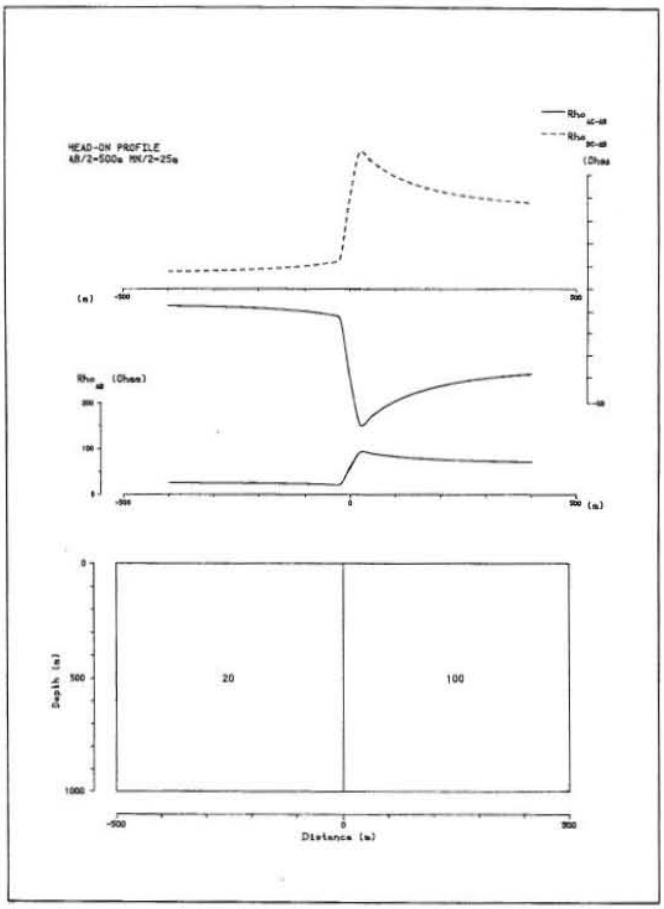

Fig. 4.8 Head-on and Schlumberger profiles over a vertical boundary

5.INTERPRETATION OF HEAD-ON DATA FROM OLKARIA,KENYA

5.1 Introdution

In 1981, head-on measurements were made by the author along several profiles in Olkaria geothermal field, Kenya. The aim was to investigate whether the head-on method could viably be used to detect fracture zones, their dip direction and the amount of dip which could greatly assist in siting geothermal wells. The measurements were made at the recommendation of the scientific review meeting (Kenya Power Company, 1980). The profiles were located close to exploration drill sites. These sites have been located near assumed faults. The head-on data from one of the profiles, HD, was sent to the Geothermal Institute at Auckland University for analysis. Unfortunately, a suitable model could not be obtained (Sudarman, pers. comm., 1982). The same profile has been reinterpreted by the author using a modifed 2-D program, DIM2K, at the Orkustofnun, Iceland. Due to lack of adequate time, this was the only profile interpreted from Olkaria.

5.2 Local Geology

The geology of the Olkaria geothermal field comprises Quaternary volcanics. These are mainly comenditic and rhyolitic lava flows and domes, and large volumes of pumiceous pyroclstics erupted from central volcanoes and vents (Nyalor, 1972; Noble and Ojiambo, 1976). North-south faults are predominant but several northeast-southwest trending faults exist, the most being the Ololbutot fault. The Ololbutot fault is seismically active. Several phreatic pumice explosions have occured. The latest eruption culminated with the recent Ololbutot flow of pumiceous obsidian (Fig.5.1) which is considered to be 300-400 years old (Naylor, 1972). The boreholes in the

JHD-HSI -9000-M.M.
82.09.1165-I.S.

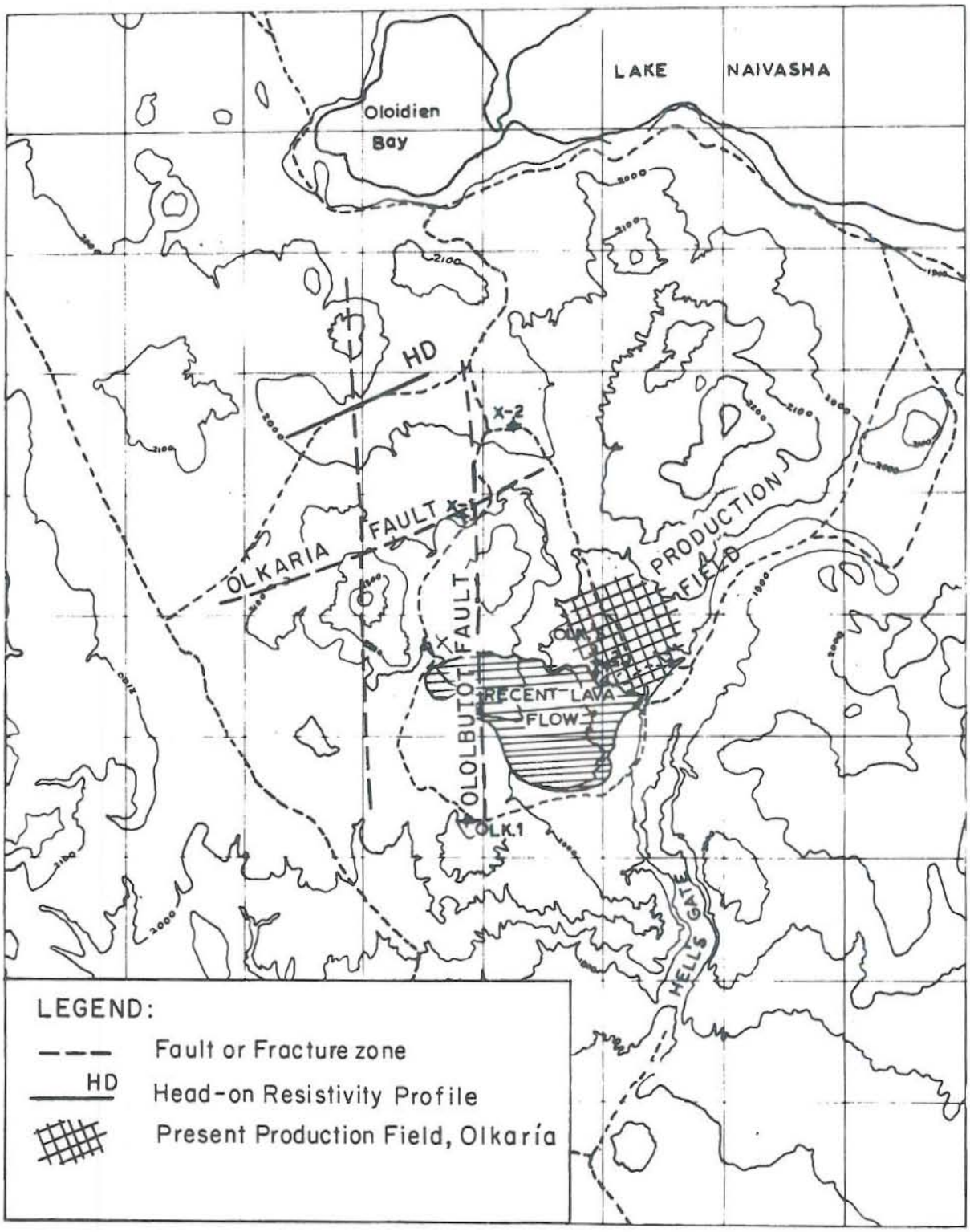

Fig. 5.1 Map of Olkaria showing faults and the location of head-on profile

present geothermal field reveal the presence of tuffs, lake beds and lava flows in the top 400m. Below this depth the strata is characterized by trachytes at 400-500m, basalts and pyroclastics at 500-700m, rhyolites at 700-800m, and trachytes, rhyolites and basalts at 800-1300m (Browne, 1981). The producing zones are found at 600-800m depth in the steam zone, and 800-900m and 1000-1100m in the liquid dominated part of the reservoir.

5.3 Head-on and gravity measurements

Profile HD is located 80 metres from exploration well 101. It is 1000m long across an assumed fracture (Fig.5.1). Head-on stations were 100m apart. The measurements were made with AB/2=250m and 500m with MN/2=24m in both cases. The fifth electrode, C, was kept at 2km. Later, it was found necessary to conduct more measurements with a larger spacing. This was done with AB/2=800m, MN/2=100m and electrode C at 3.2km. Two Schlumberger soundings were expanded at both ends of the profile with electrode spacings of AB/2=1000m. Three more soundings with AB/2=350m were made in between the long ones. The later measurements were taken during the drilling of well 101 and the readings were found to fluctuate, probably due to leakage currents from the rig. However, the readings considered here were thought to be satisfactory. The soundings were intended to provide the intitial model. The data is given in Appendix III.

Gravity measurements were made along the same head-on traverse using a Scintrex CG Gravity Meter with a sensitivity of 1 g.u. Twenty five stations were occupied along a 1.4km long line. Between stations 0 and 300W, where

the head-on data indicated a possible occurence of a fracture, the measurements were made after every 20m. Free air and Bouger corrections were made for 1900m altitude using a density of 2.0 g/ccm. Since the profile was on a relatively flat ground the topographical correction was not necessary. The data is given in Appendix IV.

5.4 Interpretation

The Schlumberger soundings were interpreted using CIRCLE2 program. The resulting section is given in Fig.(5.2) and the fitted curves in Appendix IV. A thin layer of 3-20 ohmm exists in the uppermost 50m and is not shown in the section.

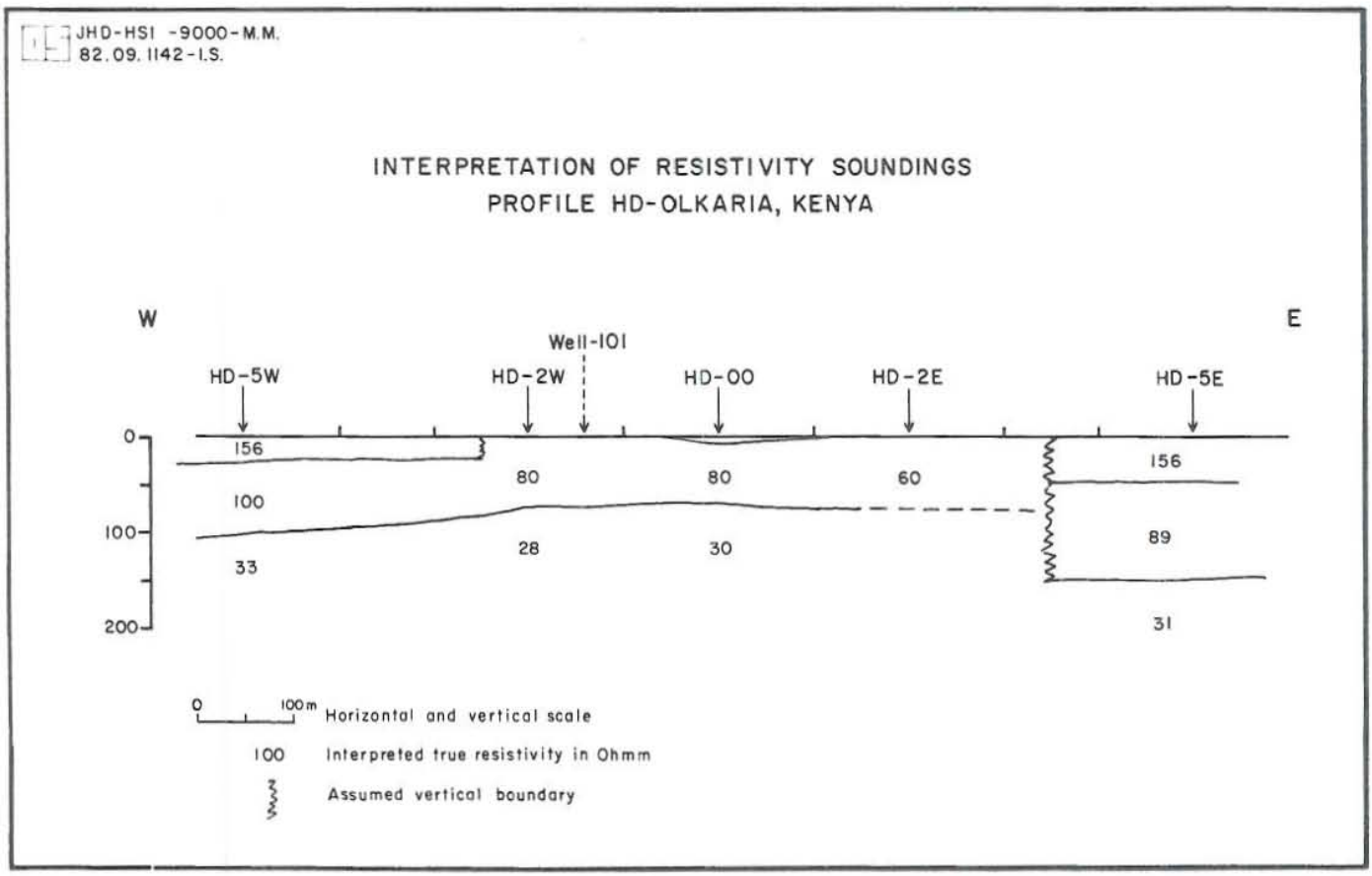

Fig. 5.2. Resistivity section interpreted from Schlumberger soundings

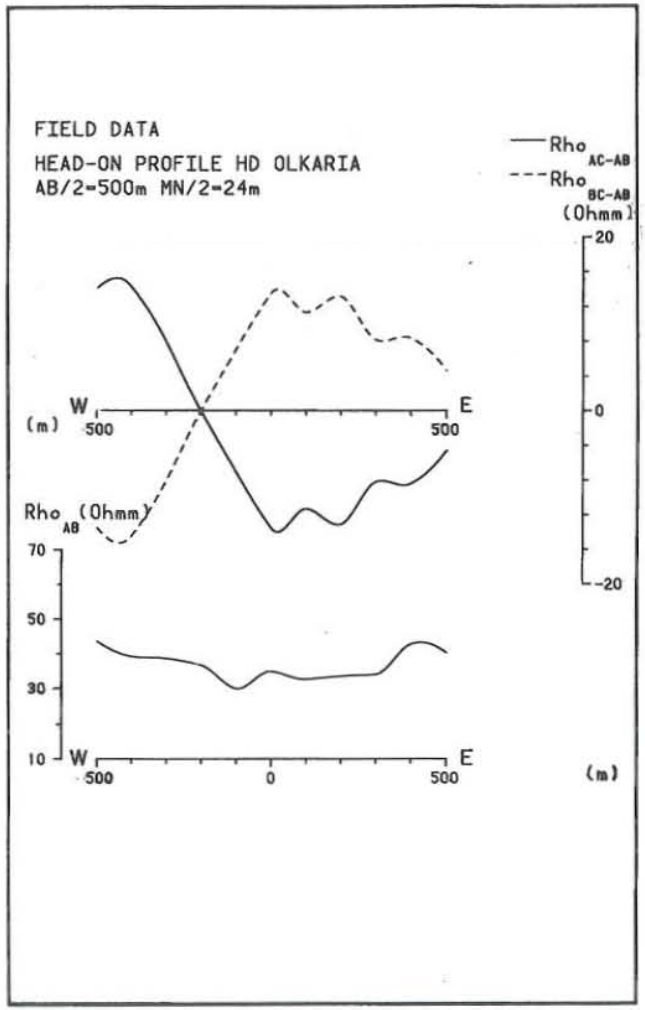

Fig. 5.3 Head-on model for AB/2=500m

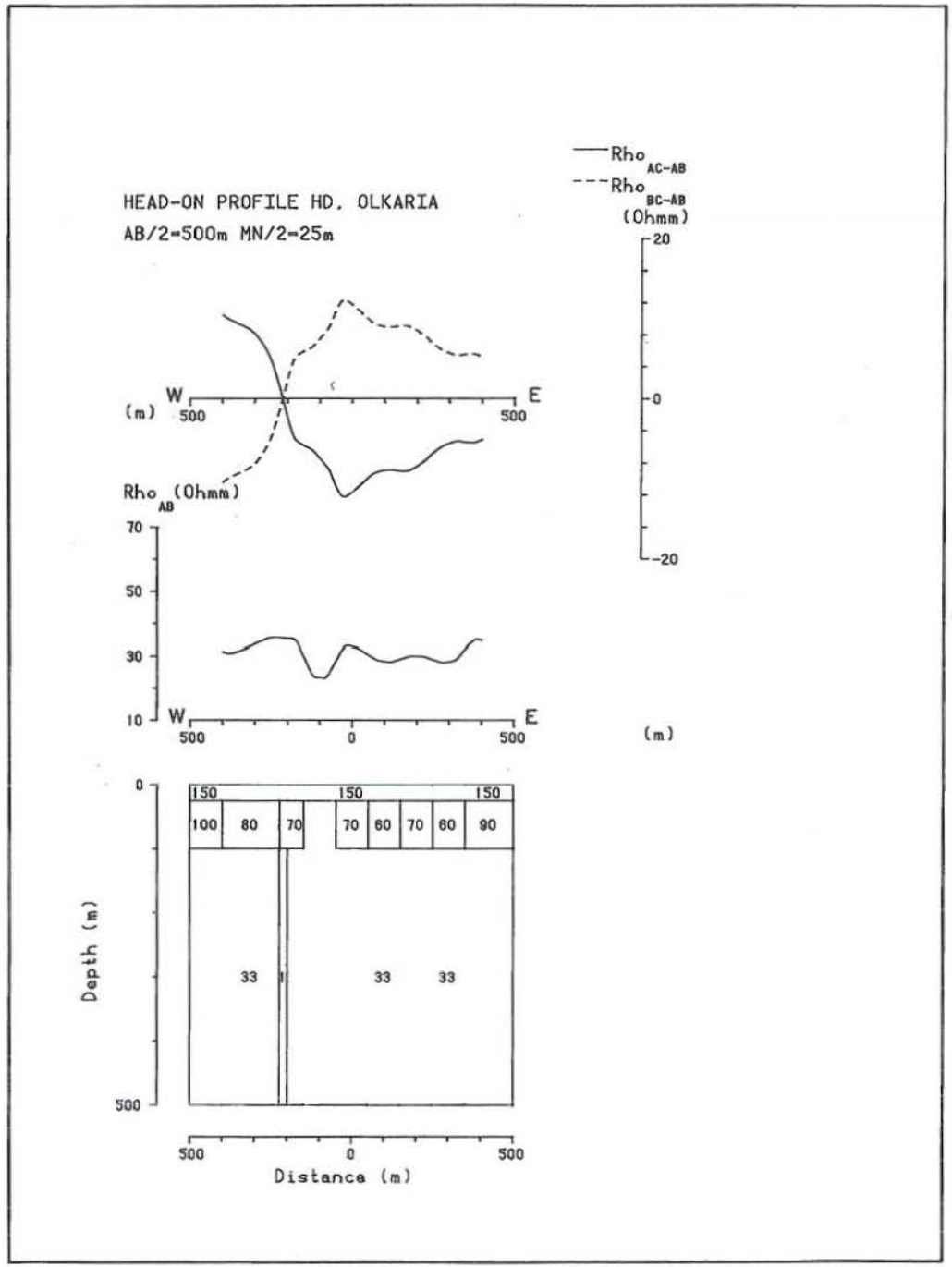

The head-on data was modelled two-dimensionally using DIM2K program. The results of the 1-D intrepretation were used as an initial model. The Shlumberger profiles were obtained from the head-on resistivities because they had not been measured separately in the field. The head-on data for AB/2=500m was modelled first and then the model modified for AB/2=250 and 800m. Since the Schlumberger profile is a measure of lateral and vertical resistivity changes, the layer parameters in the model were changed to fit it. On the other hand, the resistivity contrasts between the vertical boundaries were varied to change the amplitudes of the head-on profiles. A 1 ohmm and 25m thin vertical structure was placed near station 200W to cause the crossover. A reasonable fit was obtained, with the crossover at the same place in the model as in the field data (Fig.5.3).

For AB/2=250m, the data appeared to have been affected greatly by a nearsurface conductive layer which is evident from the Schlumberger soundings. This layer could have reduced the depth of penetration considerably. This required great changes to be made on the model of AB/2=500m if a fit was to be obtained. However, the crossover near station 1W could not be caused by the same structure modelled in AB/2=500m since it is not possible to shift this crossover even by a dipping structure. The crossover was modelled by a nearsurface low resistivity structure (see Fig.5.4). On the whole, the model profiles could not fit the field data very well, but at least they(computed profiles) explain the crossover.

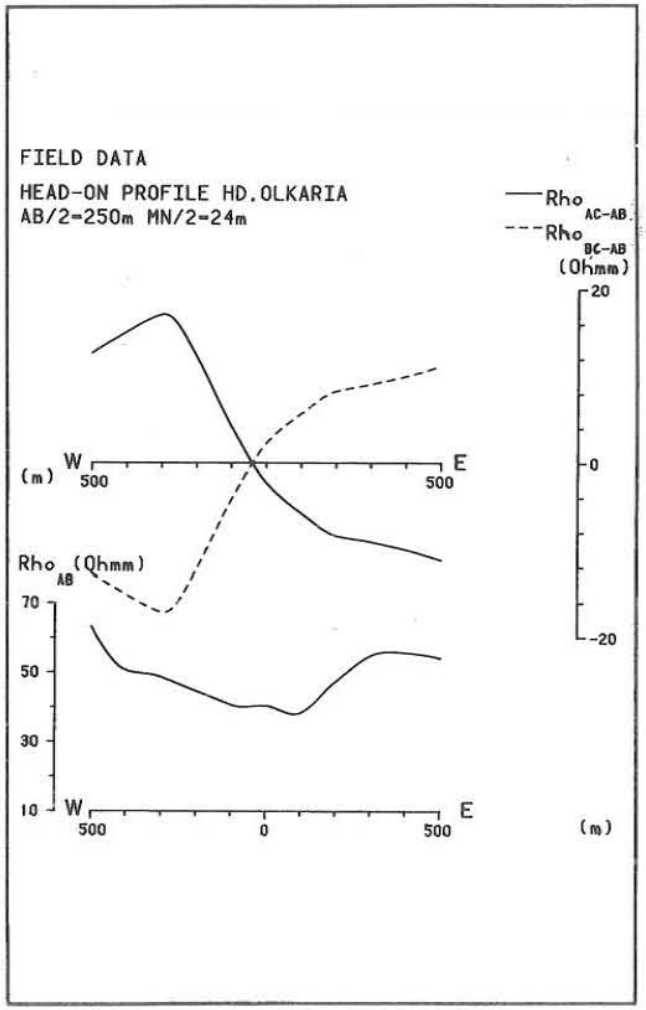

Fig. 5.4 Head-on model for AB/2=250m

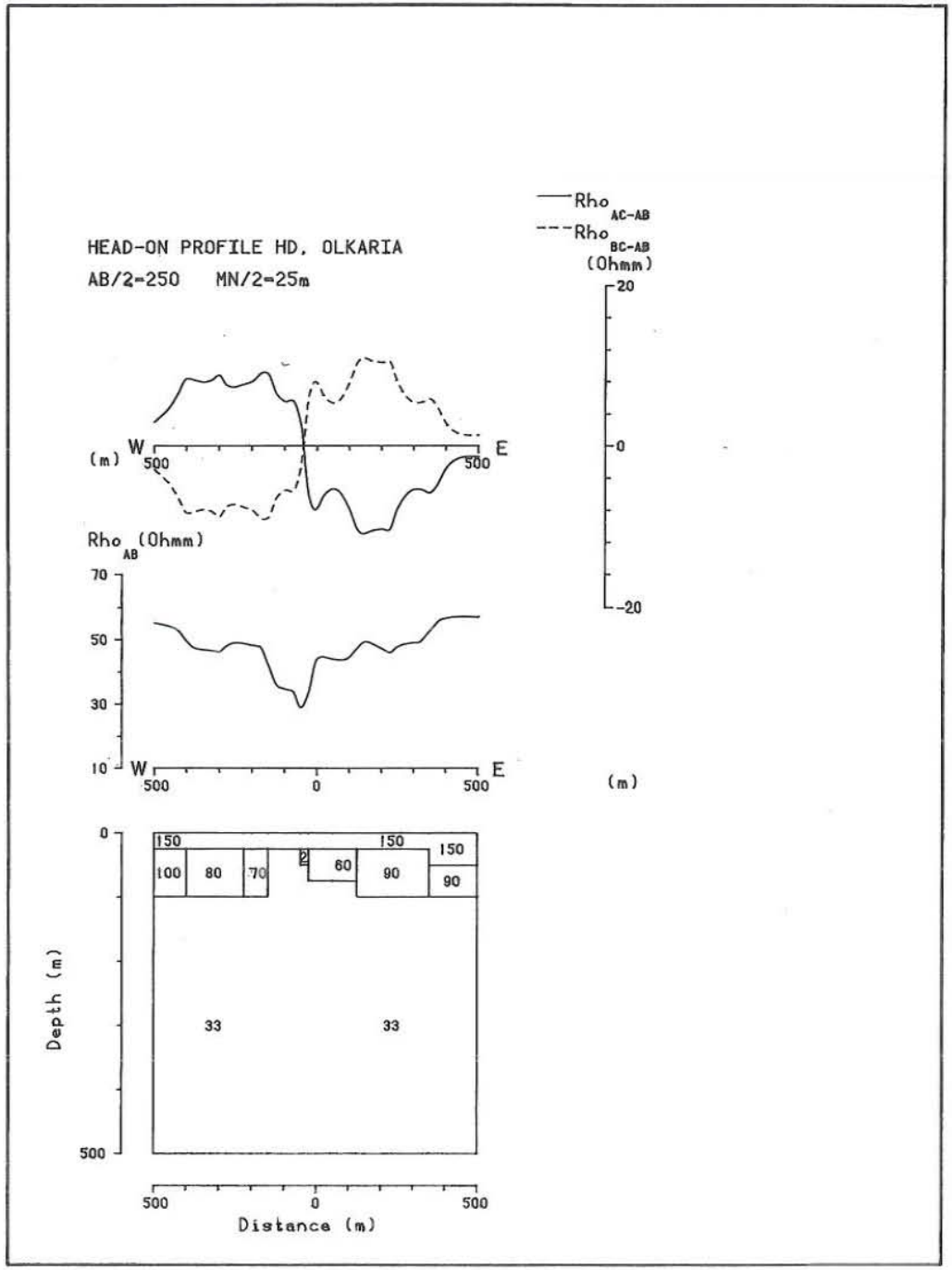

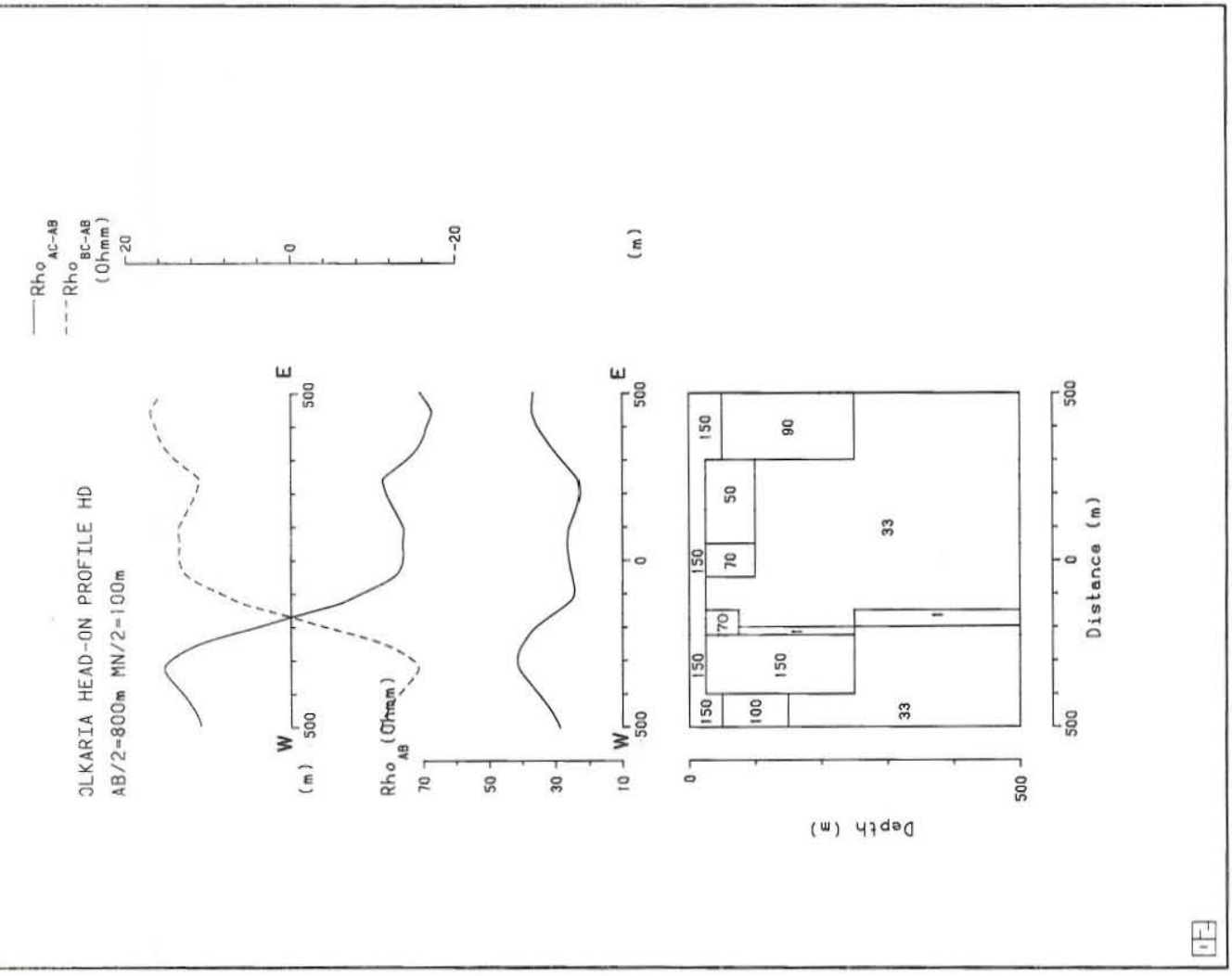

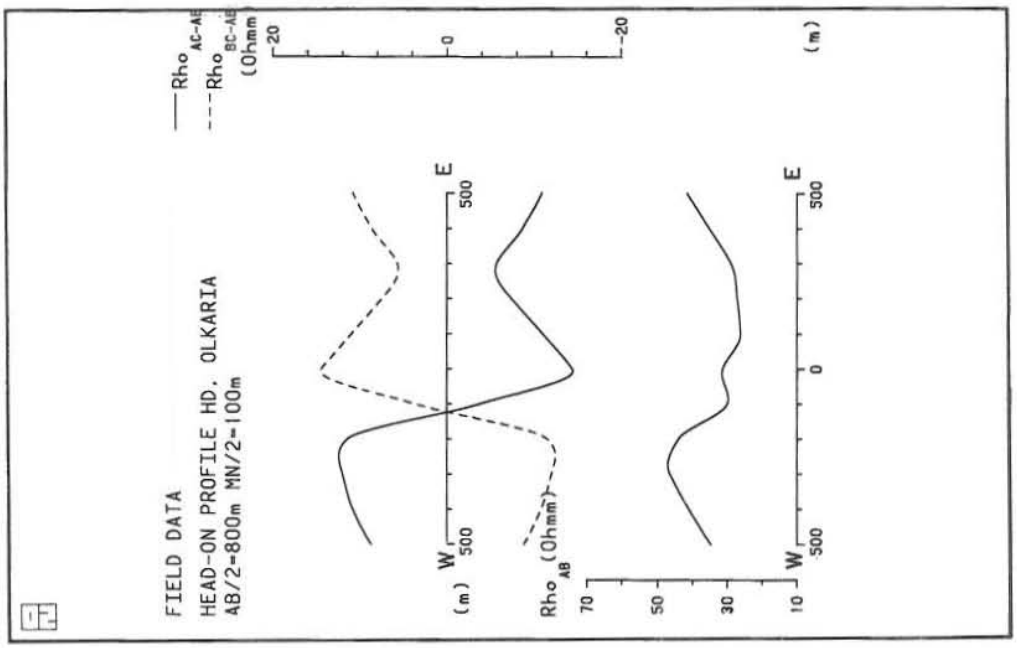

Fig. 5.5 Head-on model for AB/2=800m

The model obtained for AB/2=800m is shown in Fig.(5.5). Although the model is not bad, the crossover is slightly to the west of the field data. The resistivity and thickness of the block under station 300W had to be increased considerably in order to shift the crossover from station 200W towards station 100W as in the field data. A dipping conductive dike was tried with no success. It is probable that the crossover is indeed caused by the same low resistivity structure as for AB/2=500m, but the shift to the east is due to extremely high resistivity. This apparent high resistivity could possibly have been created by leakage currents from the rig drilling near station 100W at the time of the measurements. The part of the dike below 250m was modelled slightly to the east of station 200W (see Fig.5.5) and this could not shift the crossover and is not significant. It is most probable that the structure is approximately vertical.

The interpreted model of the gravity data is shown in Fig.(5.6). A 2-D gravity model was used assuming a regional of 2.0 g/ccm and an anomaly density of 2.3 g/ccm, which is reasonable for rhyolitic lavas in Olkaria. The computed anomaly fits the field data well.

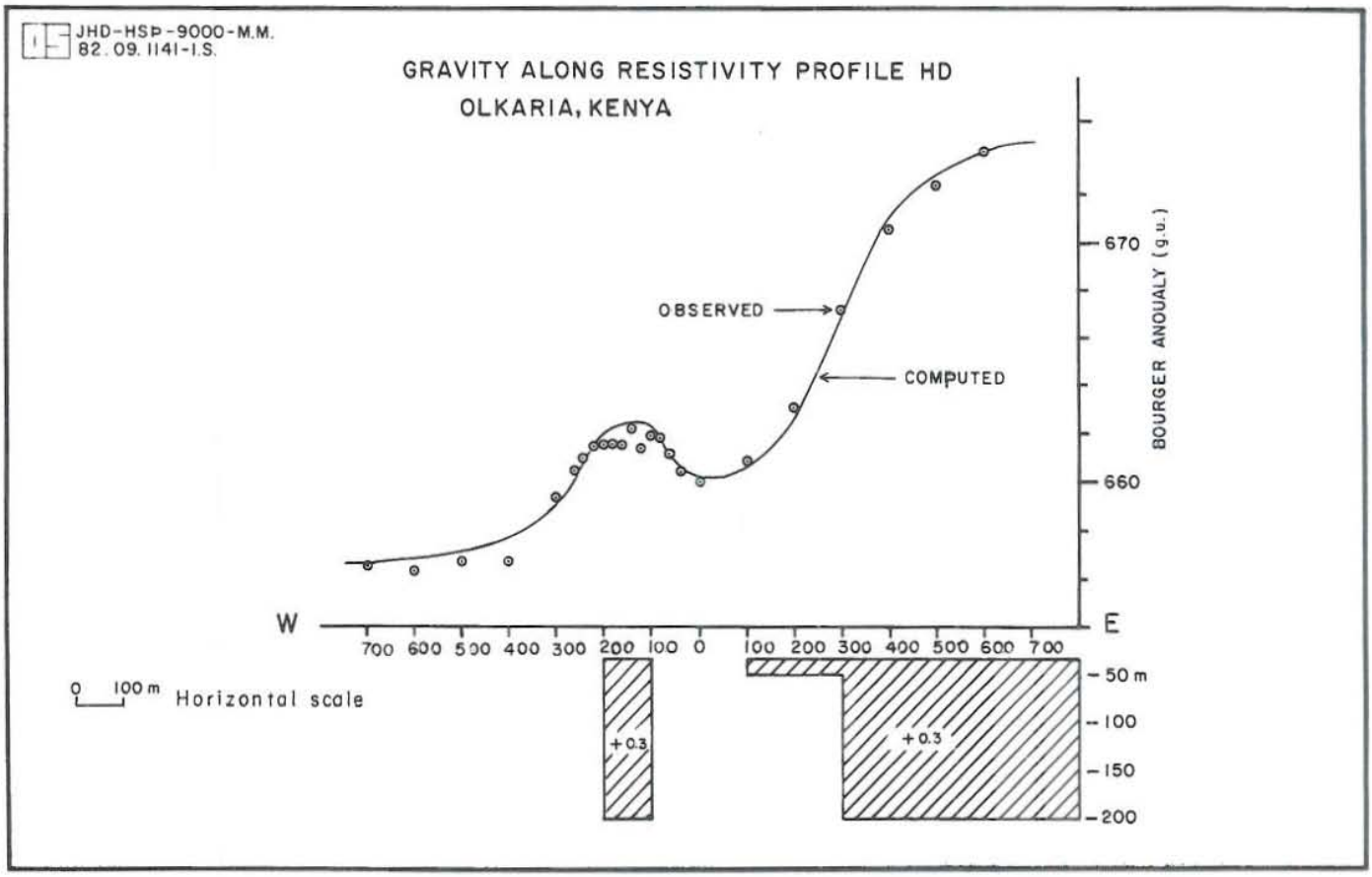

Fig 5.6 Gravity model

5.5 Discussion

The model for AB/2=250m (Fig.5.4) is probably too venerable to near surface inhomogeneities and the probing depth is shallow due the conductive layer (about 10m thick) defined by the sounding data. The crossover near station 100W is caused by a shallow conductive material.

The AB/2=500m model (Fig.5.3) is perhaps the most reliable model. The thicknesses of the layers are probably overestimated. The part of the model east of station 100W is comparable to the the gravity model, particulary the 90 ohmm layer. The 1 ohmm resistivity zone causing the crossover at station 200W has probably too low a resistivity. Because of equivalance, it could have higher resistivity and the structure thinner.

The data for AB/2=800m (Fig.5.5) is rather unreliable because the measurements must have been affected by leakage currents generated by the rig operating at the time of measurements thus creating a temporary high resistivity zone near station 300W. However, provided the unrealistic 150 ohmm layer at 300W is ignored, this model supports the existence of the low resistivity structure as in the model for AB/2=500m.

The consistent denser mass of rock east of station 2E found in gravity and resistivity models is probably a rhyolitic lava flow 100-150m thick. This continues to the south where it outcrops. The structure between stations 100W and 200W is probably a rhyolite plug. Seemingly, the gravity model does not support the presence of a fault near the conductive structure causing the crossover at deeper levels.

5.6 Conclusions

The head-on data from profile HD in Olkaria has been two-dimensionally modelled. A vertical conductive narrow zone at station 200W is responsible for the crossovers in the head-on data. It is most likely that this structure is the conduit of weak fumaroles that existed about 100m to the north of of the resistivity profile probably in the strike direction of the structure. This could also mean that well 101 could not intersect the structure. More head-on measurements to the south of profile HD are, therefore, necessary in order to confirm and trace this structure further south before any other well is drilled in this area. This work has clearly demontrated that it is possible to interpret the head-on data by two-dimesional modelling. The task should seriously be undertaken to interpret the rest of the data particulary that collected across the main Ololbutot fault.

ACKNOWLEDGEMENTS

I wish to acknowledge the following persons: Brynjolfur Eyjolfsson,who supervised the work in this report; Axel Bjornsson and Ingvar B. Fridleifsson for their very active part in the geothermal training and reading the manuscript; The lecturers at the United Nations University; Sigurjon Asbjornsson and Solveig Jonsdottir, who took care of us during our stay in Iceland; All those people at the National Energy Authority and Iceland as a whole, who helped me in a great many ways.

The gravity data was collected with the assistance of Dr J.C.Swain of Unversity of Nairobi whom I owe special gratitude.

I am grateful for the award of the United Nations Fellowship,1982.

The East African Power and Lighting Company,Kenya,gave me the subertical leave which I would like to acknowledge.

Thanks to the United Nations Univeristy fellows for a wonderful time together.

REFERENCES

Apparao,A.,Roy,A., and Mallick,K.,1969: Resistivity model experiments. Geoexploration, 7,45.

Beyer,J.H.,1977: Telluric and D.C. resistivity techniques applied to the geophysical investigation of Basin and Range Geothermal Systems, Part II: A numerical study of the dipole-dipole and Schlumberger resistivity methods. Ph.D. Thesis,LBL,6325 2/3.

Bjornsson,A,1981, Exploration and exploitation of low-temperature geothermal fields for district heating system in Akureyri, North Iceland.Geothermal Resources Transactions, 5, 495-498.

Bjornsson,A.and Saemundsson,K.,1975: Geothermal areas in the vicinity of Akureyri.A report of the National Energy Authority,Iceland. OSJHD 7557 (In Icelandic).

Browne,P.R.L.,1981: Petrographyic study of cuttings from ten wells drilled at the Olkaria Geothermal field, Kenya. Geothermal Institute of Auckland, NZ. A report for Kenya Power Company.

Cheng,Y.W.,1980: Location of nearsurface faults in geothermal prospects by "combined head-on resistivity profiling method". Proceedings of the New Zealand Geothermal workshop, 1980, 163-166.

Dey,A.,1976: Resistivity modelling for arbitrarily shaped two-dimensional structures Part II: User's guide to the FORTRAN algorithm RESIS2D. LBL-5283.

Dey,A. and Morrison,H.F.,1979: Resistivity modelling for arbitrarily shaped two-dimensional structures. Geophys.Prospect., 27,106-136.

Flovenz,O.G. and Eyjolfsson,B.,1981: Resistivity soundings an estimate of geothermal areas in Eyjafjördur. National Energy Authority report, Iceland, OS81029/JHD17 (in Icelandic with English summary).

De Gery,J.C. and Kunetz,G.,1956: Potential and resistivity over dipping beds. Geophysics, 21,780-793.

Johansen,K,1977: A man/computer system for interpreting resistivity soundings over a horizontal stratified earth. Geophys.Prospect., 25,667-691.

Koefoed,O.,1979: Geosounding Principles 1: Resistivity sounding measurements. Elsevier, Amsterdam, 276.

Kenya Power Company,1980: Minutes for Scientific Review Meeting 1 - 5 Dec., 1980. Unpublished Geothermal Project report.

Lee,T.,1981: Direct interpretaion of resistivity data over two-dimensional structures. Geophys.Prospect., 29, 462-469.

McPhar Geophysics,1967: Catalogue of resistivity and IP model data. McPhar Geophysics Ltd., Ontario, Canada.

Naylor,W.I.,1972: The geology of Eburru and Olkaria geothermal prospects. Unpublished report for UNDP/EAPL Geothermal Exploration Prospects.

Noble J.W.and Ojiambo,S.B.,1976: Geothermal Exploration in Kenya. Second UN Geothermal Proc.,(Lawrence Berkeley Lab., Calif.), 189-204.

Unz,M.,1953: Apparent resistivity curves for dipping beds. Geophysics, 18, 116-137.

Van Nostrand,R.G. and Cook,K.L.,1956: Apparent resistivity for dipping beds-a discussion. Geopysics, 20,140-147.

AK152 MODEL 1

INPUT VALUES

NO. OF X-POINTS= 113 NO. OF Z-POINTS= 16 NO. OF FILTERP.= 9

XSCAL= 1.00 ZSCAL= 1.00 UNIT=25.00

DISTANCES BETWEEN LINES

IN X-DIRECTION (DX) :

1000.00	100.00	20.00	4.00	1.00	1.00	1.00	1.00
1.00	1.00	1.00	1.00	1.00	1.00	1.00	1.00
1.00	1.00	1.00	1.00	1.00	1.00	1.00	1.00
1.00	1.00	1.00	1.00	1.00	1.00	1.00	1.00
1.00	1.00	1.00	1.00	1.00	1.00	1.00	1.00
1.00	1.00	1.00	1.00	1.00	1.00	1.00	1.00
1.00	1.00	1.00	1.00	1.00	1.00	1.00	1.00
1.00	1.00	1.00	1.00	1.00	1.00	1.00	1.00
1.00	1.00	1.00	1.00	1.00	1.00	1.00	1.00
1.00	1.00	1.00	1.00	1.00	1.00	1.00	1.00
1.00	1.00	1.00	1.00	1.00	1.00	1.00	1.00
1.00	1.00	1.00	1.00	1.00	1.00	1.00	1.00
1.00	1.00	1.00	1.00	1.00	1.00	1.00	1.00
1.00	1.00	1.00	1.00	4.00	20.00	100.00	1000.00

IN Z-DIRECTION (DZ) :

1.00	1.00	1.00	1.00	2.00	2.00	2.00	2.00
2.00	2.00	4.00	4.00	8.00	64.00	512.00	

VALUES OF FILTERPOINTS:

0.006	0.009	0.020	0.050	0.090	0.150	0.300	0.600
1.250							

NO. OF TRANSMITTING POINTS= 20 NO. OF RECEIVING POINTS= 2
X-NUMBER OF CENTER OF ARRAY= 57 ANGLE = 0.0 DEGREES

X-NUMBERS OF TRANSMITTING POINTS (ITX) :

15	19	23	27	31	35	39	43
47	51	63	67	71	75	79	83
87	91	95	99				

COEFFICIENTS FOR HOMOGENEOUS EARTH :

1.019	1.010	1.004	0.997	0.988	0.976	0.962	0.946
0.928	0.908						

X-NUMBERS OF RECEIVING POINTS (IRX) :

55	59

RESISTIVITY STRUCTURE

NO. OF X-BLOCKS : 5

NO. OF LAYERS : 3

LAYER 1 RESISTIVITY : 350.0 THICKNESS : 100.0 DEPTH : 100.0
LAYER 2 RESISTIVITY : 40.0 THICKNESS : 200.0 DEPTH : 300.0
LAYER 3 RESISTIVITY : 100.0

X-BOUNDARY 1 : -850.0

NO. OF LAYERS : 4

LAYER 1 RESISTIVITY : 150.0 THICKNESS : 25.0 DEPTH : 25.0
LAYER 2 RESISTIVITY : 40.0 THICKNESS : 50.0 DEPTH : 75.0
LAYER 3 RESISTIVITY : 80.0 THICKNESS : 225.0 DEPTH : 300.0
LAYER 4 RESISTIVITY : 120.0

X-BOUNDARY 2 : -50.0

NO. OF LAYERS : 4

LAYER 1 RESISTIVITY : 70.0 THICKNESS : 25.0 DEPTH : 25.0
LAYER 2 RESISTIVITY : 3.0 THICKNESS : 175.0 DEPTH : 200.0
LAYER 3 RESISTIVITY : 80.0 THICKNESS : 100.0 DEPTH : 300.0
LAYER 4 RESISTIVITY : 120.0

X-BOUNDARY 3 : 100.0

NO. OF LAYERS : 4

LAYER 1 RESISTIVITY : 70.0 THICKNESS : 25.0 DEPTH : 25.0
LAYER 2 RESISTIVITY : 20.0 THICKNESS : 175.0 DEPTH : 200.0
LAYER 3 RESISTIVITY : 80.0 THICKNESS : 100.0 DEPTH : 300.0
LAYER 4 RESISTIVITY : 120.0

X-BOUNDARY 4 : 500.0

NO. OF LAYERS : 3

LAYER 1 RESISTIVITY : 275.0 THICKNESS : 100.0 DEPTH : 100.0
LAYER 2 RESISTIVITY : 20.0 THICKNESS : 150.0 DEPTH : 250.0
LAYER 3 RESISTIVITY : 480.0

CALCULATED CURVE

AB/2= 150.00 RHOAPP= 14.8517
AB/2= 250.00 RHOAPP= 11.4313
AB/2= 350.00 RHOAPP= 11.1359
AB/2= 450.00 RHOAPP= 11.4327
AB/2= 550.00 RHOAPP= 14.5093
AB/2= 650.00 RHOAPP= 18.4209
AB/2= 750.00 RHOAPP= 16.8573
AB/2= 850.00 RHOAPP= 18.5798
AB/2= 950.00 RHOAPP= 18.4351
AB/2= 1050.00 RHOAPP= 18.1726

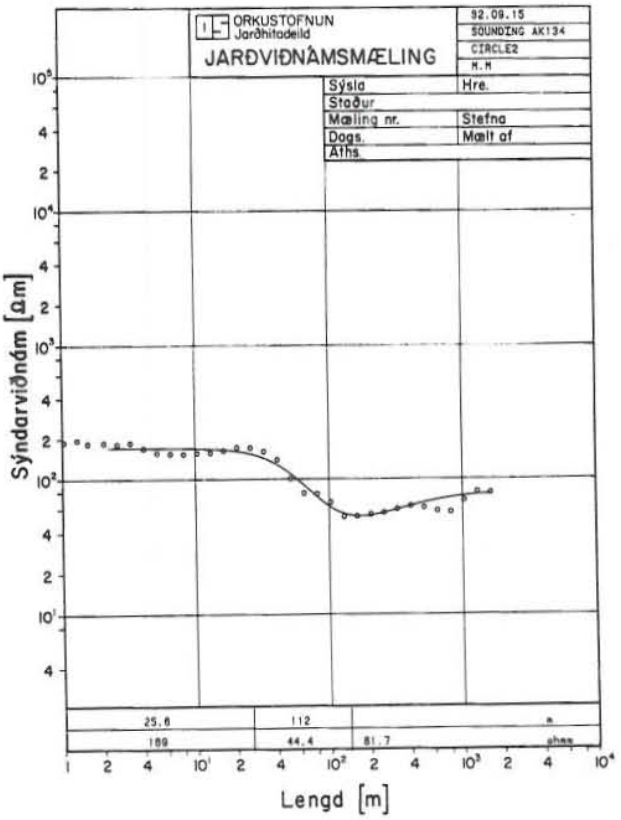
ORKUSTOFNUN
Jarðhitadeild
JARÐVIÐNÁMSMÆLING
82.09.15
SOUNDING AK134
CIRCLE2
H.H
Sýsla
Hre.
Staður
Mæling nr.
Stefna
Dags.
Mælt af
Aths.
Sýndarviðnám [Ωm]
Lengd [m]

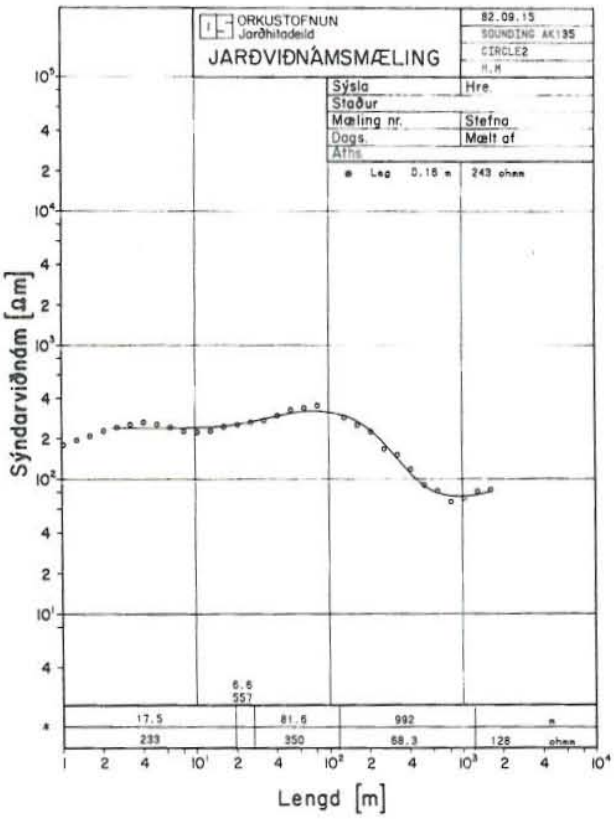
ORKUSTOFNUN
Jarðhitadeild
JARÐVIÐNÁMSMÆLING
82.09.15
SOUNDING AK135
CIRCLE2
H.H
Sýsla
Hre.
Staður
Mæling nr.
Stefna
Dags.
Mælt af
Aths.
Sýndarviðnám [Ωm]
Lengd [m]

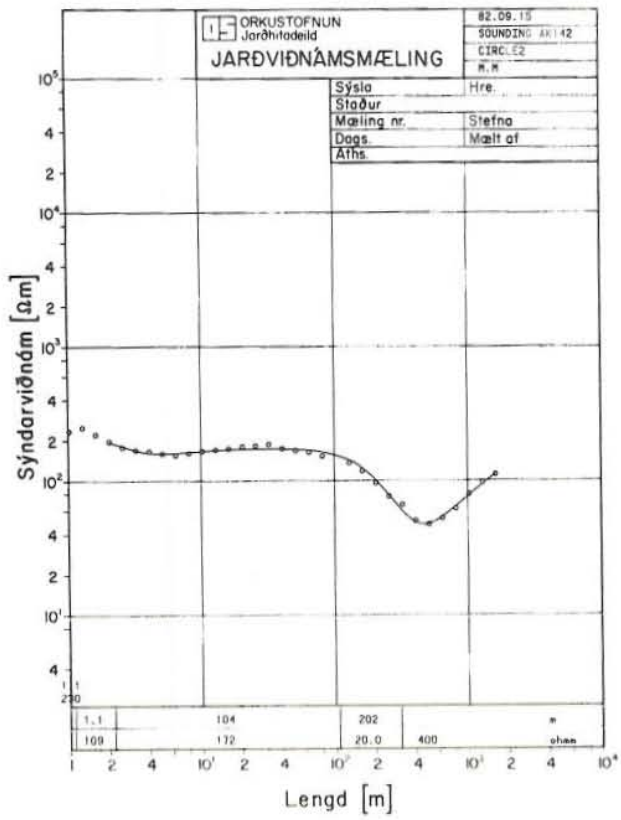
ORKUSTOFNUN
Jarðhitadeild
JARÐVIÐNÁMSMÆLING
82.09.15
CIRCLE2
H.H
Sýsla
Hre.
Staður
Mæling nr.
Stefna
Dags.
Mælt af
Aths.
Sýndarviðnám [Ωm]
Lengd [m]

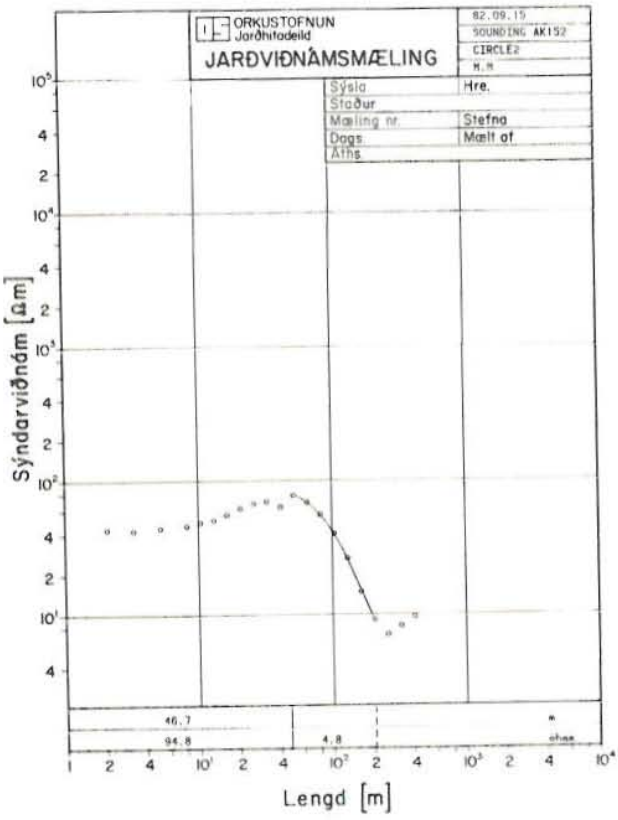
ORKUSTOFNUN
Jarðhitadeild
JARÐVIÐNÁMSMÆLING
82.09.15
CIRCLE2
H.H
Sýsla
Hre.
Staður
Mæling nr.
Stefna
Dags.
Mælt af
Aths.
Sýndarviðnám [Ωm]
Lengd [m]

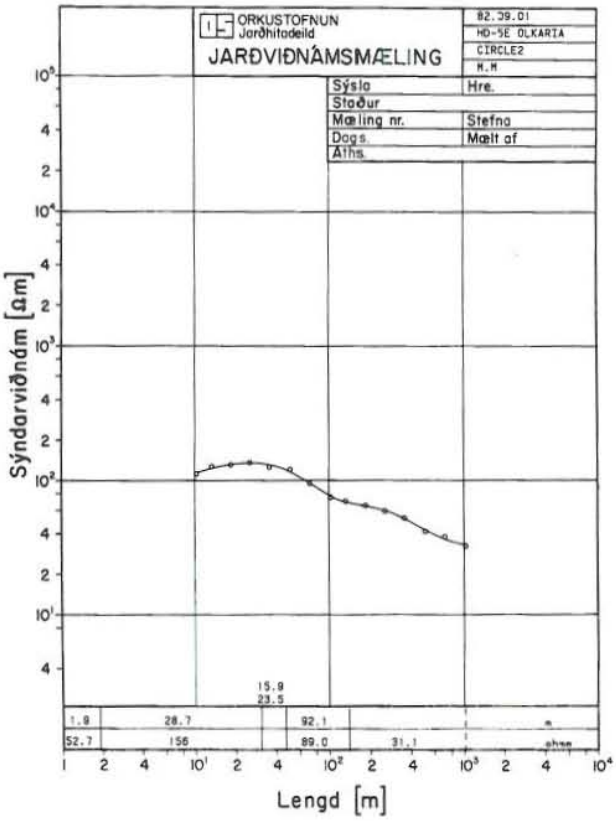
ORKUSTOFNUN
Jarðhitadeild
JARÐVIÐNÁMSMÆLING
82.09.01
HD-5E ÖLKARIA
CIRCLE2
H.H
Sýsla
Hre.
Staður
Mæling nr.
Stefna
Dags.
Mælt af
Aths.
Sýndarviðnám [Ωm]
Lengd [m]
15.9
23.5
1.9
28.7
92.1
52.7
156
89.0
31.1
ohm

PROFILE HD, OLKARIA

HEAD-ON DATA AB/2=250m MN/2=24m

ST	Rho AC	Rho BC	Rho AB
500W	76.0	50.7	63.4
400W	65.7	35.5	50.6
300W	65.7	31.5	48.6
200W	56.8	32.4	44.6
100W	44.8	36.4	40.6
0.00	38.0	42.6	40.3
100E	32.4	43.9	38.2
200E	38.8	55.5	47.2
300E	45.6	63.8	54.7
400E	45.6	65.6	55.6
500E	42.8	65.2	54.0
AB/2=500m MN/2=24m			
500W	57.6	30.1	43.6
400W	53.5	24.8	39.2
300W	46.6	30.6	38.6
200W	36.7	36.7	36.7
100W	22.9	36.9	29.9
0.00	21.4	48.4	34.9
100E	21.3	43.9	32.6
200E	20.4	46.6	33.5
300E	25.8	42.1	34.0
400E	34.3	51.0	42.7
500E	35.7	44.9	40.3
AB/2=800m MN/2=100m			
500W	43.4	25.9	34.7
400W	51.8	30.2	41.0
300W	58.5	34.5	46.5
200W	55.5	32.6	44.1
100W	26.2	33.8	30.0
0.00	16.9	45.7	31.3
100E	15.2	37.1	26.2
200E	19.8	34.6	27.2
300E	23.2	34.6	28.9
400E	26.4	43.7	35.5
500E	30.6	52.3	41.5

OLKARIA GRAVITY DATA PROFILE HD

CORRECTED FOR HEIGHTS ABOVE 1900m
DENSITY USED =2.0 g/cm cu.
STATIONS NAMED BY THEIR DISTANCES FROM STATION 0

STATION	LEVELS(m)	HEIGHTS(m)	GRV.(gu)	DRIF.CR	(h*2.248)	B.A (gu)
700W	1990.248	90.248	455.6	453.7	202.9	656.6
600W	1990.185	90.185	455.5	453.6	202.7	656.3
500W	1990.225	90.225	455.7	453.9	202.8	656.7
400W	1990.140	90.140	455.9	454.1	202.6	656.7
300W	1991.868	91.868	453.6	451.9	206.5	658.4
260W	1991.019	91.019	456.5	454.8	204.6	659.4
240W	1988.293	88.293	464.1	462.5	198.5	661.0
220W	1986.952	86.952	467.6	466.0	195.5	661.5
200W	1986.688	86.688	468.1	466.6	194.9	661.5
180W	1986.102	86.102	469.5	468.0	193.6	661.6
160W	1985.394	85.394	471.0	469.5	192.0	661.5
140W	1985.024	85.024	472.5	471.1	191.1	662.2
120W	1984.569	84.569	472.7	471.3	190.1	661.4
100W	1984.448	84.448	473.5	472.1	189.8	661.9
80W	1984.239	84.239	473.7	472.4	189.4	661.8
60W	1984.059	84.059	473.45	472.15	189.0	661.2
40W	1983.797	83.797	473.3	472.0	188.4	660.4
0	1983.144	83.144	474.3	473.1	186.9	660.0
100E	1981.474	81.474	479.5	477.7	183.2	660.9
200E	1978.514	78.514	488.4	486.6	176.5	663.1
300E	1974.901	74.901	500.5	498.8	168.4	667.2
400E	1971.071	71.071	512.4	510.8	159.8	670.6
500E	1970.146	70.146	516.2	514.7	157.7	672.4
600E	1968.616	68.616	512.0	519.6	154.2	673.8
700E	1966.956	66.956	526.1	524.8	150.5	675.3

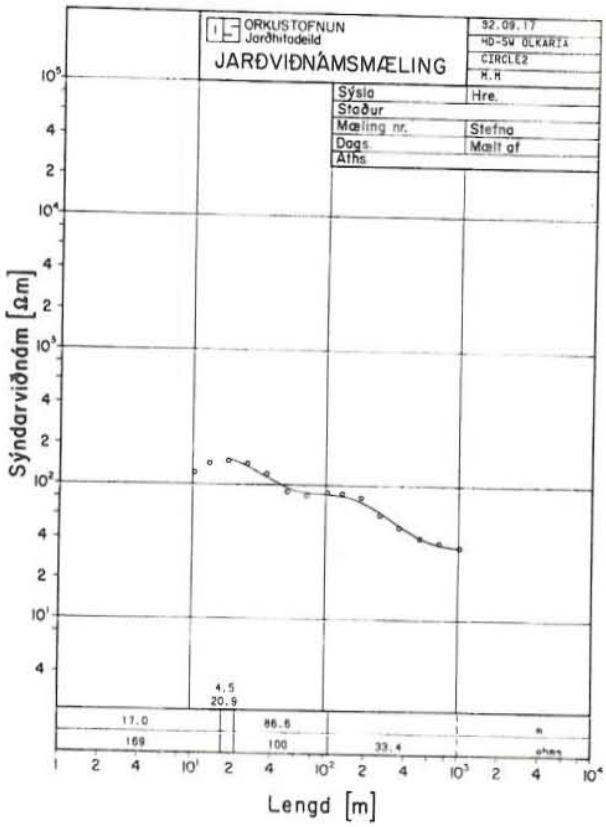
ORKUSTOFNUN
Jarðhitadeild
JARÐVIÐNÁMSMÆLING
82.09.17
HD-5W OLKARIA
CIRCLE2
M.H
Sýsla
Hre.
Staður
Mæling nr.
Stefna
Dags.
Mælt af
Aths
Sýndarviðnám [Ωm]
Lengd [m]
4.5
20.9
17.0
169
86.6
100
33.4
ohm

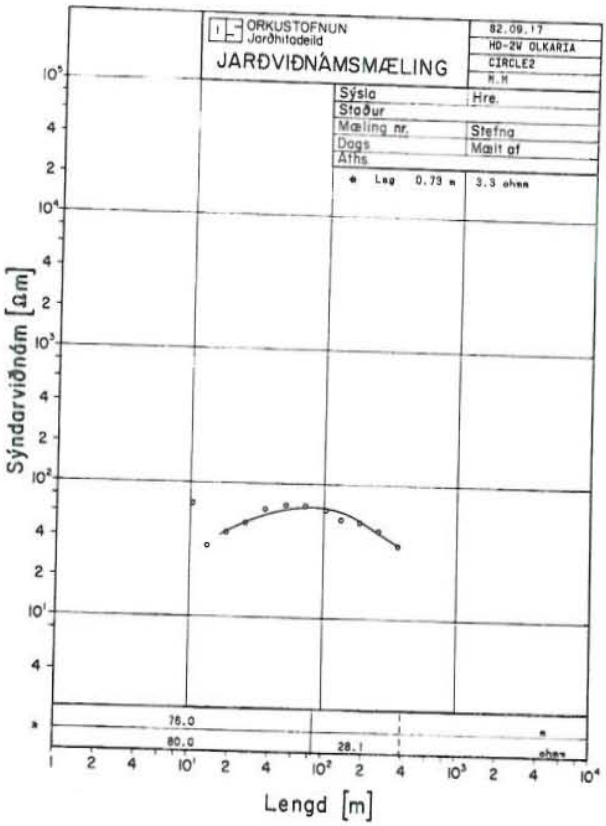
ORKUSTOFNUN
Jarðhitadeild
JARÐVIÐNÁMSMÆLING
82.09.17
HD-2W OLKARIA
CIRCLE2
M.H
Sýsla
Hre.
Staður
Mæling nr.
Stefna
Dags
Mælt af
Aths
Lag 0.73 m 3.3 ohm
Sýndarviðnám [Ωm]
Lengd [m]
78.0
80.0
28.1
ohm

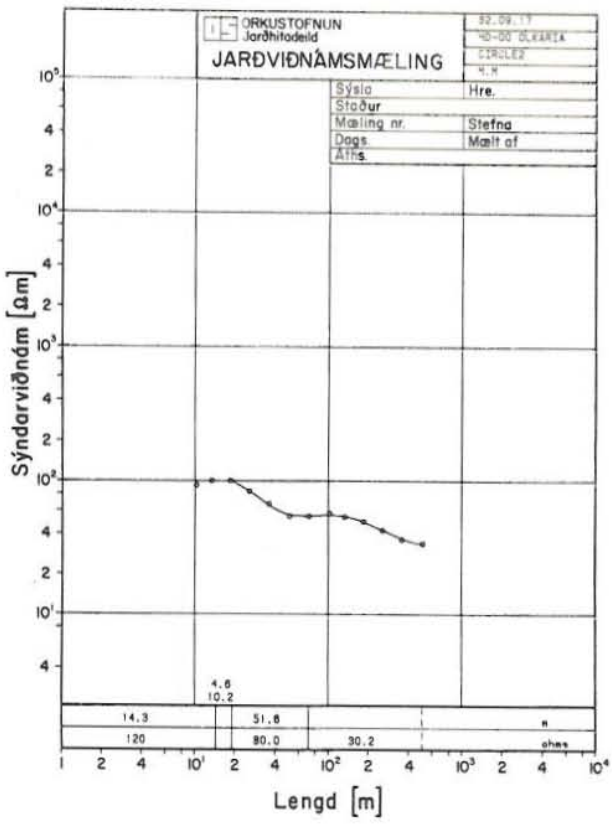
ORKUSTOFNUN
Jarðhitadeild
JARÐVIÐNÁMSMÆLING
82.09.17
HD-00 OLKARIA
CIRCLE2
M.H
Sýsla
Hre.
Staður
Mæling nr.
Stefna
Dags.
Mælt af
Aths.
Sýndarviðnám [Ωm]
Lengd [m]
4.6
10.2
14.3
120
51.8
80.0
30.2
ohm

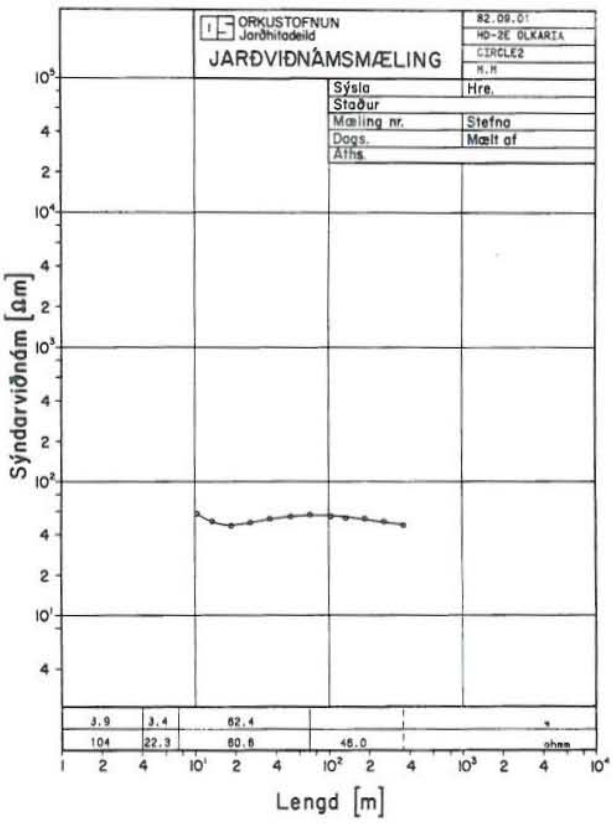
ORKUSTOFNUN
Jarðhitadeild
JARÐVIÐNÁMSMÆLING
82.09.01
HD-2E OLKARIA
CIRCLE2
M.H
Sýsla
Hre.
Staður
Mæling nr.
Stefna
Dags.
Mælt af
Aths.
Sýndarviðnám [Ωm]
Lengd [m]
3.9
104
3.4
22.3
62.4
80.6
46.0
ohm

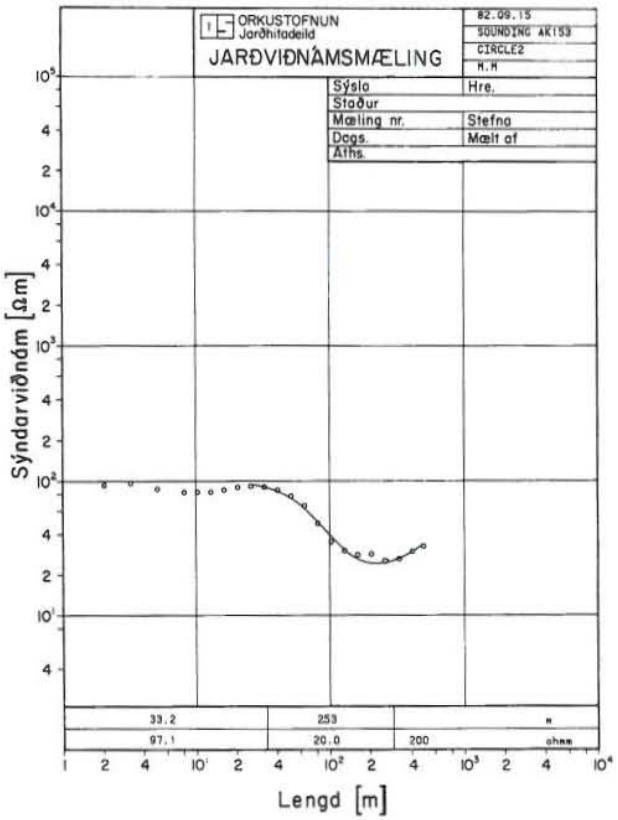
ORKUSTOFNUN
Jarðhitadeild
JARÐVIÐNÁMSMÆLING
82.09.15
SOUNDING AK153
CIRCLE2
H.H
Sýsla
Hre.
Staður
Mæling nr.
Stefna
Dags.
Mælt af
Aths.
Sýndarviðnám [Ωm]
Lengd [m]
33.2
97.1
253
20.0
200
ohmm